Research Paper

Part-load thermal efficiency enhancement in gas turbine combined cycles by exhaust gas recirculation

Mohammad Ali Motamed [a,*], Magnus Genrup [b], Lars O. Nord [a]

[a] *Department of Energy and Process Engineering, Norwegian University of Science and Technology—NTNU, Trondheim, Norway*
[b] *Department of Energy Sciences, Lund University, Lund, Sweden*

ARTICLE INFO

ABSTRACT

Gas turbine power plants are popular for offshore power generation due to high power density and their reliability. However, growing usage of renewable energies put gas turbines in a load following backup operation. These power plants suffer part-load efficiency losses when operating at less than full capacity, resulting in higher carbon dioxide (CO_2) emission from natural gas combined cycles or higher consumption of carbon-free fuels in decarbonized gas turbines. In this article, a solution is proposed for enhancement of power plant part-load thermal efficiency based on exhaust gas recirculation in the gas turbine cycle. Recirculating exhaust gas into the gas turbine have been studied by several researchers and engineers due to its benefit for carbon-free combustion and carbon capture mechanisms. The proposed operation strategy is evaluated for single-spool and two-spool gas turbines operating jointly with a steam bottoming cycle harvesting the waste heat for further power production. In the suggested strategy, eliminating the necessity to cool down the recirculated gas resulted in less equipment footprint for the power plant which makes it more favorable for offshore applications. An in-house design and simulation tool is developed for evaluating gas turbines with modern gas recirculating systems and a flexibility in operation with carbon-free fuel mixtures. The enhancement in efficiency boost, emission reduction, and fuel consumption is quantified demonstrating the improvements with the proposed solution.

1. Introduction

Norway has set the ambition to become a low-emission society by 2050 [1]. This is considered a contribution to the Paris agreement and Europe's emission goals. An extensive effort is seen to reach climate neutrality which is mostly focused on carbon dioxide (CO_2) emission reduction in the offshore oil and gas industry. Investigations showed that on the Norwegian continental shelf (NCS), more than 12 million tons of equivalent CO_2 originated from offshore petroleum activities in 2021 [2]. It is translated to nearly a quarter of Norway's total CO_2 emissions [3]. Norway is considered one of the pioneers in developing low carbon intensity petroleum activities. The authorities introduced a CO_2 tax scheme as early as 1991 [4]. The tax regime is kept increasing to push the operators for having a cleaner oil production. In 2020, the cost of CO_2 emission is estimated to NOK 700-800 per ton of CO_2 on the NCS [5].

In recent years, there has been a growing trend towards incorporating renewable energy sources in several power sectors including the oil and gas industry. Renewables reached a 40% share of total installed power capacities around the world in 2022 [6]. A total of 295 GW of renewables were installed around the world in 2022, which was a record in yearly installation of renewables [6]. This shift towards renewables is driven by several factors, including increasing pressure to reduce greenhouse gas emissions from fossil fuels, rising energy costs of low carbon fuels or carbon free fuels, and technological advancements that have made renewable energy more affordable and accessible. As a measure for more affordable renewable energy production, data from 2020 shows a continuous decline of electricity generation cost, falling 9% and 13% annually for offshore and onshore wind respectively [7]. The use of renewable energy in the oil and gas industry can take many forms but mostly includes use of wind turbines to generate electricity for power and process. Europe target for 300 GW of offshore wind installations, which is 12 times larger than offshore wind turbines installed by end of 2020 [8]. However, it is expected that onshore wind turbines will have higher market value in future whereas offshore wind turbines are unlikely to be a commercially viable technology in Norway in 2040 [9]. On the other hand, offshore wind turbines are considered an alternative in the platforms that are located far from shore [10]. By adopting renewable energy solutions, the oil and gas industry has

Nomenclature

Abbreviations

EGR	exhaust gas recirculation
EGT	exhaust gas temperature
IGV	inlet guide vane
NOK	Norwegian kroner
TIT	turbine inlet temperature
FHV	fuel heat value (lower heat value)

Notations

A	heat exchanger effective area (m^2)
C	heat capacity (J/K)
$\vec{E}$	error vector
F	pressure loss factor
f	friction factor
f_{IGV}	IGV correction factor
$f_{scaling}$	scaling correction factor
H	enthalpy (J)
k	thermal conductivity (W/mK)
M	performance map parameter
MW	molecular weight (mol/gr)
$\dot{m}$	mass flow rate (kg/s)
n	number of gas turbine units
N	rotational speed (rad/s)
Nu	Nusselt number
P	Power (W)
p	pressure (Pa)
$\bar{R}$	universal gas constant (J/molK)
Re_D	Reynolds number based on the diameter
T	temperature (K)
U	overall heat transfer coefficient (W/m^2K)
V	volume (m^3)
$\vec{V}$	guessed variables vector
X	Parson number
y_{mean}	mean steam wetness (kg/kg)

Greek letters

α	Baumann factor
β	auxiliary coordinate in the performance map
$\bar{\beta}$	heat transfer coefficient ratio
Δ	parameter change
ϵ_D	relative surface roughness
η	efficiency
Π	pressure ratio
ρ	density (kg/m^3)
ϕ	fuel air ratio
Ω	burner loading parameter

Subscripts

air	related to air
amb	ambient conditions
bur	related to burner
c	corrected
cc	combined cycle
cold	heat exchanger cold side
comp	related to compressor
dp	design point
dry	dry expansion
f	gas turbine fuel
GT	related to gas turbine
hot	heat exchanger hot side
HP	high pressure turbine
IGV	related to inlet guide vane
in	inlet
L	large
LP	low pressure turbine
map	related to performance map
max	maximum
mech	mechanical
min	minimum
out	outlet
s	isentropic
S	small
ST	steam turbine
t	total
th	thermal
turb	related to turbine
wet	wet expansion

reduced its environmental impact, improved operational efficiency, and increased its long-term sustainability. As an example, a 200,000 tons per year CO_2 emission cut is expected from the oil field by installing 11 wind turbines (total of 88 MW capacity) in Norway's Hywind Tampen project [11].

A significant challenge of using wind energy as a power source in the oil and gas industry is its intermittent availability, which can result in significant fluctuations in power output. The amount of electricity generated by a wind turbine drop significantly when the wind speed falls below 60% of its maximum speed [12]. To address this issue, gas turbines are often used as backup load systems to maintain a stable power supply during periods of low wind availability. The rapid load management capability of gas turbines makes them an attractive choice for compensating load fluctuations in wind turbines [13]. However, a significant amount of heat is lost in the exhaust gas of gas turbines, which reduces the overall efficiency of the system. To address this issue, gas turbines are often combined with a steam bottoming cycle, which harnesses the waste heat from the gas turbine and uses it to generate additional power. This combined cycle configuration results in a significant increase in energy efficiency, with some systems achieving efficiencies of over 60% [14]. The combination of gas turbines and steam bottoming cycles is an effective way to improve the energy efficiency of

power generation systems and reduce their environmental impact.

Part-load operation of gas turbines can significantly impact performance, efficiency, and emissions from the combined cycle. Combined cycle performance may decline because of two factors, reduced gas turbine efficiency, and decrease in the amount of heat accessible to the steam cycle. Thermal efficiency of the gas turbine at 30% load may drop to 60% or less of the efficiency from the design point [15]. This reduction in gas turbine efficiency resulted in a 30% less overall efficiency of the combined cycle [16]. Inefficient operation at part-load increases gas turbine specific fuel consumption to over 20% higher than design value [17]. The second factor negatively impacting cycle efficiency at part-load is reduced heat available to the steam cycle which is initiated by less gas turbine mass flow rate and less exhaust temperature. 40% less exhaust mass flow rate and 30% lower exhaust temperature can be expected at 50% load resulting in 15% less combined cycle efficiency [18,19].

In offshore application where reliability is of higher priority, gas turbines spend a majority of their operational lifespan in part-load operation with poor energy efficiency. Two gas turbines may share 50% of the load while a third one remains at standby in case of need [20]. In addition, offshore gas turbines may tailor their design to ensure reliability in penalty of inefficient performance [21]. Therefore, part-

load enhancement has a potential to result in significant cost savings and CO_2 emission cut. It would facilitate a reliable and efficient integration of wind energy into power generation systems in the oil and gas industry.

The Exhaust Gas Temperature (EGT) from a two-spool gas turbine decreases when operating at low power levels. This will deteriorate combined cycle efficiency in gas turbine and steam cycle configuration since less heat is available to the bottoming cycle [22]. Keeping gas turbine exhaust temperatures high at reduced loads or even increasing the EGT in single-spool gas turbines is introduced as a solution to enhance combined cycle efficiency. It provides higher energy transfer to the heat recovery steam generator, which can result in increased steam production and ultimately, more electricity generation. Several techniques can be employed to modify exhaust temperature during partial load conditions and enhance the overall performance of the combined cycle system.

The conventional approach to control EGT of single-spool gas turbines at part-load involves the utilization of variable geometry blades in the compressor entry rows. These pivoted blades allow for regulation of the mass flow rate, effectively controlling the exhaust temperature during part-load operation. Haglind showed in [23] that combined cycle part-load efficiency can be improved by 10% in a variable guide vane control strategy relative to a fixed geometry single-spool gas turbine. However, this method is not effective at low power loads. The variable guide vane controller struggles to maintain a consistent exhaust temperature when operating at loads below 40%. This is because the guide vanes typically reach their maximum closure at loads below 40%–50% [24].

Compressor variable guide vanes are however not effective in controlling EGT of two-spool gas turbines [25]. Two-spool gas turbines featuring an independent power turbine are widely used in offshore applications due to wide operating range and high flexibility range [26]. One possible solution to tackle this problem is to regulate the core engine speed at part-load. Another approach to manage EGT of two-spool gas turbines at part-load is to consider incorporating variable nozzle guide vanes in the turbine inlet [27]. Variable geometry turbine blades are studied show their capability to maintain EGT at or near the full load level for power demands higher than 40% [28]. However, it can be expected that using pivoted vans in turbine hot section may be expensive and technically challenging due to high temperature condition in which the mechanical mechanism must endure long-term operation.

Recirculating gas turbine exhaust flow can be used as a method for managing EGT during partial load conditions [29]. The utilization of Exhaust Gas Recirculation (EGR) in gas turbines is anticipated to increase due to its numerous advantages in promoting decarbonized solutions, particularly in the areas of carbon capture systems and hydrogen combustion solutions [30,31]. When a high rate of EGR is used, combustion air has a significantly reduced amount of oxygen, which helps keep the flame temperature at stoichiometric levels low, thus preventing the formation of high levels of Nitrogen Oxides (NO_x) [32]. Moreover, hydrogen fired gas turbines can tolerate higher EGR rates relative to natural gas fired engines due to higher flame speed and higher reactivity [33]. EGR may be sued as a strategy to overcome the challenges associated with achieving reduced levels of NO_x emissions when burning fuels with high hydrogen content in gas turbines [34]. EGR can also result in decreased energy usage in a CO_2 capture system by taking advantage of the elevated concentration of CO_2 in the flue gas [35]. A case study investigating the improvement of post-combustion CO_2 capture plant showed that the specific reboiler duty in a chemical absorption process can be decreased by 9% through an exhaust gas recirculation process [36]. The significance of this becomes more pronounced when considering that the concentration of CO_2 in flue gas decreases significantly during partial load operation [18]. A comparison of carbon capture enhancement is conducted in [37] between two-spool and single-spool gas turbines when working with high EGR ratio. It showed that the two-spool gas turbine had a higher improvement in

carbon capture performance due to increased CO_2 concentration. In addition, the number of absorber trains will be reduced due to lower volume flow rate of the flue gas [30]. Qureshi et al. showed that this could reduce the gas flow rate through the CO_2 absorber by 70% compared to conventional fresh air combustion in a case study resulting in smaller absorber diameter [38]. The reduction in equipment footprint will help make carbon capture systems more feasible for offshore applications where space is limited, and compactness is a primary consideration.

EGR can reduce risk of equipment degradation and enhance combustion stability in decarbonized combined cycle power plants in case of partial load operation. Lower oxygen concentration at recirculated flue gas reduces amine degradation and the corrosion phenomena related to the oxygen by-products in the carbon capture facilities [39]. Furthermore, maintaining a high EGT by using EGR can enable the steam turbine to function at high temperatures, potentially mitigating the chances of degradation and extending the operational lifespan of the steam turbine.

There have been recent developments in the methods and mechanisms used for gas recirculation in combined cycles. A proof of technology feasibility is demonstrated in [40] investigating simple cycle gas turbine EGR through a practical experiment showing enhancement in heat rate, load range, and NO_x level while not affecting sound emission and durability in a 12-month period. A recent study in [41] introduced a new approach to push the limit of EGR ratio further to the range of 0.5–0.8. The EGR ratio is defined as the ratio of recirculated gas mass flow rate to the mass flow rate entering the engine. The advancement is made possible by additive oxygen injection at gas turbine inlet. However, it does not consider the combined cycle layout and the power range is limited to 50% to 100% of full load capacity. A study in [42] demonstrated that using EGR in hydrogen fired gas turbines only cause slight alterations in the operational parameters of turbomachinery components. Therefore, incorporating EGR with hydrogen-fired cycles can be achieved without significant modification of existing gas turbine equipment. In a novel research [43], the use of an ejector as a new method for exhaust gas recirculation is proposed rather than conventional methods such as using a fan or a valve. This technique involves utilizing a small amount of high-pressure air, obtained from the compressor discharge (approximately 1% of the total air intake).

The thermal efficiency of combined cycle power plants can be enhanced employing EGR to keep EGT elevated during partial load operation. This approach involves reintroducing the exhaust gas back into the gas turbine inlet, which leads to higher temperatures and helps to maintain elevated exhaust temperatures at low load demands. Effect of controlled EGT on a combined cycle performance is investigated in [44] demonstrating a potential for performance improvement by flue gas recirculation. However, the study in [44] only considers full load operation and does not include the performance improvement potential at part-load operation. The potential of part-load performance improvement by warm EGR has been investigated in [24] for single-spool gas turbine combined cycles. Nonetheless, the research conducted in [24] has certain constraints as the gas turbine inlet temperature is limited to 50 °C, leaving room for improvement. An extensively examination of warm EGR is presented in [31] for single-spool gas turbine combined cycle operating with high-volume hydrogen fuel; However, the improvement in cycle efficiency is not significant (less than one percentage point) and it does not consider a two-spool configuration.

Two knowledge gaps are identified in the research regarding the application of warm EGR for enhancement of combined cycle power plants. Firstly, two-spool gas turbines operating in combined cycles are not well studied in the open literature for part-load efficiency enhancement with warm EGR. A desire can be seen in the industry and academia to find a practical solution for regulating EGT in two-spool gas turbines without the need for modifying the design of gas turbine. It will bring benefits for combined cycle power units in oil and gas industry operating mostly in part-loads. Secondly, a comprehensive performance

investigation of single-spool gas turbines in combined cycles with warm EGR was not found in the open literature concerning operation in 40% of full load capacity or lower. Most of the existing studies have primarily been conducted within the industry, leading to a focus on practical limitations imposed by current technology. However, it is intriguing to explore a comprehensive investigation that pushes these limits, particularly with regards to future applications and the challenges associated with low load operation.

This article presents a method for enhancing the thermal efficiency of combined cycle power plants with a focus on low load operation. The proposed approach involves recirculating warm gas within the gas turbine, and the amount of recirculated gas is adjusted to optimize the overall efficiency of the combined cycle during partial load conditions. The studied thermal process involves mixing warm exhaust gas with fresh air to elevate the gas turbine inlet temperature. This method proves to be effective in regulating the combined cycle power output during part-load operation. The thermal process leverages the advantages of gas recirculation in gas turbines, such as increasing combustion stability and enhancing the efficiency of the carbon capture process. The proposed thermal process finds application in offshore decarbonized combined cycles that operate in conjunction with renewable energies. Specifically, during low-load operation, the suggested thermal process is anticipated to result in reduced CO_2 emissions and lower fuel consumption. Simultaneously, it diminishes the reboiler duty in the post-combustion carbon capture process.

The study investigates the suggested operating strategy for both single-spool and two-spool gas turbines, in combination with a steam bottoming cycle that utilizes a sliding pressure control strategy. This work's novelty lies in the use of warm gas recirculation to improve combined cycle thermal efficiency in case of two-spool gas turbines. A significant challenge tackled in this study is the comprehensive analysis of the combined cycle under part-load conditions, where simulating the gas turbine, steam cycle, and the combined cycle with recirculated exhaust gas proves to be particularly complex. What sets this study apart is its comprehensive simulation covering detailed system performance, including component efficiency, interstage thermodynamic properties, and interstage gas composition, distinguishing it from existing studies in the open literature. Another noteworthy aspect is that unlike existing solutions, this approach does not necessitate any alterations to the design of the gas turbine core engine. Consequently, it can be implemented in a retrofit process with minimal impact on existing installations. Moreover, the system exhibits robustness in terms of control strategy selection, allowing for rapid and easy transitions between conventional and novel control strategies, or a combination of both. This adaptability makes it compatible with other control strategies already in use for gas turbines and combined cycles. Furthermore, the proposed solution presents a novel approach to reduce the firing temperature in single-spool gas turbines, contributing to an extended lifespan and decreased maintenance expenses. This study goes beyond traditional considerations by evaluating lifetime performance in addition to thermodynamic performance. An additional innovation lies in the reduction of the system's footprint and size. The proposed control strategy suggests potential space savings by eliminating the need for a recirculated gas cooler, leading to not only a smaller physical footprint but also reduced energy consumption, considering the energy-intensive nature of providing cooling media.

2. Method

This section details the approach employed in developing the simulation technique utilized to evaluate the proposed design solution. Our objective was to create a digital simulation package capable of assessing the performance of combined cycles with gas turbines under diverse operating conditions. Although commercial simulation tools are accessible, they often have inherent limitations that hinder accurate evaluation of our innovative solution. In contrast, the developed tool

provides a higher degree of flexibility, allowing us to explore and implement new control strategies, thereby facilitating a more comprehensive analysis. The method employed for the development of this simulation tool is described herein. To ensure its accuracy and reliability, the tool is verified using industrial data as well as data obtained from open literature sources, thereby establishing its validity for subsequent analyses and investigations.

2.1. System configuration and layout

Fig. 1 depicts the selected arrangement design for combined cycle heat and power generation, employing two Siemens gas turbines. These turbines are utilized for producing electricity and heat simultaneously in the combined cycle setup. To guarantee swift power restoration in case of an engine shutdown, the load is evenly divided, with each turbine bearing 50% of the overall load. The extraction of process heat occurs before the bottoming cycle, ensuring that the required heat is accessible for offshore platform installations. This is particularly important because wind energy is utilized for a portion of the offshore installation's electricity needs. Thus, the entire heat required for the installation is supplied through the process heat extraction loop, making its availability crucial.

Downstream of the gas turbines, a single pressure level steam bottoming cycle is implemented to generate additional power using the exhaust heat from the gas turbines. This design choice avoids the use of multi-pressure level steam turbines, aiming for a more compact configuration suitable for offshore applications. Table 1 presents the tabulated information regarding the design characteristics of the steam cycle. To recover heat from the gas turbine exhaust, a heat recovery system is incorporated in between. For compact heat recovery in offshore settings, a once-through steam generator is suggested as a promising technology, offering the advantage of minimal space footprint [45,46]. An axial multistage steam turbine configuration is assumed to extract power from the superheated steam due to high power to size ratio. The water pressurization is facilitated by a variable frequency drive (VFD) pump. The variable speed pump enables the cycle to operate at varying pressure levels, accommodating fluctuations in load demand during partial-load conditions. This sliding pressure control strategy proves to be an efficient method for regulating power output when the available heat level from the gas turbine is reduced [47].

The proposed operational strategy entails redirecting warm discharge gas back into the gas turbine inlet through a recirculation process, which occurs after the bottoming cycle. A booster fan is used to facilitate this recirculation. In low loads, it is possible to extract a portion of the exhaust gas from the gas turbine discharge and mix it with
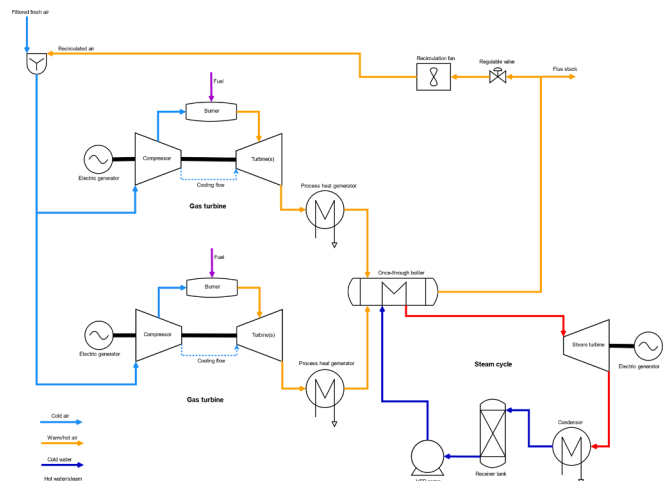

Fig. 1. Combined cycle layout configuration.

Table 1

Steam cycle specifications.

Specifications	Value	Specifications	Value
pinch point temperature difference	10 °C	condenser pressure loss	5%
steam turbine efficiency	80%	heat recovery unit pressure loss	5%
pump efficiency	70%	process heat	10 MW

the recirculated gas. This mixing process serves to increase the enthalpy of the recirculated gas without exceeding the limit of 50% gas recirculation ratio. The recirculated gas and fresh air are then mixed prior to entering the gas turbines.

2.2. Component performance model

To evaluate the system's performance under various operating conditions, it is crucial to possess a reliable model for its components. The model used strives for maximum inclusivity since limited geometric information is accessible during the initial design evaluation phase. This approach ensures the model's versatility in accommodating various technological options.

Gas turbine, heat recovery system, the bottoming cycle, and recirculation circuit are broken down into their primary components. The thermodynamic properties of the working fluid are assessed at each interstage station. The key components such as the compressor, turbine, and heat exchanger are considered as black boxes, utilizing generalized performance models. By understanding the thermodynamic state of the working fluid at each interstage, performance metrics of the system can be computed for the given operational conditions.

The COOLPROP software library is employed for the computation of gas mixture and steam thermodynamic properties [48]. Air is considered as a gas mixture composed of five components: Oxygen, Nitrogen, Carbon dioxide, Argon, and water vapor with associated humidity. The fuel consists of a combination of natural gas components (Methane, Ethane, and Propane), Ammonia, and Hydrogen, with the specific mixture composition determined by the user. In the bottoming cycle, the working fluid is regarded as pure water in different states, including subcooled, superheated, and two-phase conditions.

Compressor: The gas turbine receives air through an intake system, which is considered an adiabatic component. The intake system has a user-defined pressure loss factor. The air is then compressed in the compressor, taking into account the isentropic efficiency that considers irreversibility in the process. The isentropic efficiency of the compressor is defined by equation (1).

$$\eta_{comp,s} = \frac{H_{out,s} - H_{in}}{H_{out} - H_{in}} \tag{1}$$

In which, H is enthalpy of the gas in the station. According to dimensional analysis, the compressor pressure ratio and isentropic efficiency are determined using the compressor corrected speed, which is calculated as $(N_c = \frac{N\sqrt{MW}}{\sqrt{RT}})$ and the inlet corrected mass flow rate, calculated as $(\dot{m}_c = \frac{\dot{m}\sqrt{RT_t}}{P_t\sqrt{MW}})$ [49]. The corrected speed and corrected mass flow rate depend on the compressor inlet temperature, pressure, and gas composition. A performance map of an axial compressor, presented in [50], is chosen as a general reference. The generic map is then scaled using the scaling factors presented in equation (3) to match the design values defined by the user. Additionally, correction factors specified by the user are incorporated to address any performance changes resulting from the adjustment of the variable inlet guide vanes (IGVs) (equation (4). Subsequently, all performance indicators (M) in the compressor map are modified according to the scaling factor and the IGV correction factor (equation (2). In an operational point, the proximity of the operation

point to a highly risky surge operation is quantified by the compressor surge margin (equation (5).

$$f_{scaling} = \frac{M_{dp}}{M_{dp,map}@\beta_{dp}} \tag{2}$$

$$f_{IGV} = \frac{dM}{dIGV°} \tag{3}$$

$$M = M_{map} * f_{scaling} * f_{IGV}; \quad M \equiv \dot{m}_c, (\Pi - 1), \eta_{comp,s} \tag{4}$$

$$Surge\ margin = \frac{\Pi_{surge} - 1}{\Pi - 1} \frac{\dot{m}_c}{\dot{m}_{c,surge}}@const.speed \tag{5}$$

Interpreting the compressor performance map poses a mathematical challenge due to the nearly vertical constant speed lines. This makes it difficult to extract data from the tabulated performance map. To overcome this challenge, a method suggested in [51] is applied, which involves introducing an auxiliary coordinate β (Fig. 2). The power consumed by the turbine is evaluated according to the enthalpy rise across the compressor.

Burner: The burner is considered an adiabatic chemical reactor with a pressure loss determined by the user. Equation (6) presents the overall form of the chemical reaction equation. The volumetric composition of the products is calculated according to chemical balance of the chemical elements (H, C, O, N, Ar) in the reaction. Knowing burner discharge temperature, the energy conservation balance is used to calculate the fuel-air ratio based on the enthalpy of reactant and products. To account for deviations from ideal complete combustion in the actual combustion process, a burner efficiency is introduced. In off-design conditions, the deviation in burner efficiency is modelled based on the burner loading parameter (equation (7). The burner loading is defined in equation (8) and is calculated based on inlet condition to the burner, burner inlet mass flow rate, and the burner volume [52].

$$\phi[(C_{H4} + C_2H_6 + C_3H_8) + H_2 + NH_3] + Air \rightarrow N_2 + O_2 + Ar + H_2O + CO_2 \tag{6}$$
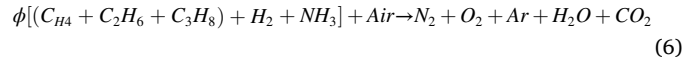
$$\frac{1 - \eta}{1 - \eta_{dp}} = \left(\frac{\Omega}{\Omega_{dp}}\right)^{1.6} \tag{7}$$

$$\Omega = \frac{\dot{m}_{in}}{V_{bur}p_{in}^{1.8}e^{T_{in}/300K}} \tag{8}$$

Turbine: The mechanical power in the turbine is generated through the expansion of high-temperature gas in the turbine blades, which converts
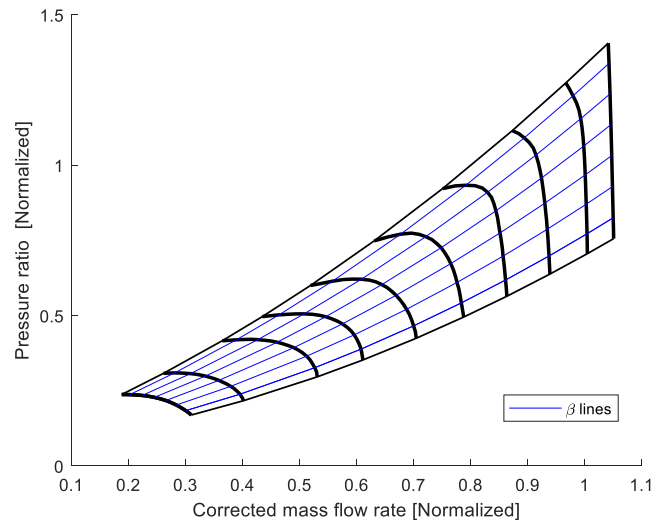

Fig. 2. Generic compressor performance map.

the thermal energy of the burned gas into usable power. To prevent overheating of the blades, a portion of the air from the compressor discharge is bled and injected at the first row of blades and vanes for cooling purposes. The mixing of the cooling air and the high-temperature air in the nozzle guide vanes and the first row of rotor blades is modelled as an adiabatic mixing process without any pressure loss. This mixing process occurs before the gas expansion takes place in the turbine blades [52]. To assess the efficiency, capacity and pressure ratio through the axial turbine, a simulation is conducted using non-dimensional parameters and a performance map method, similar to the approach outlined in the compressor section. A generic performance map from the study in [53] is selected and then scaled based on the user's provided design value. An auxiliary coordinate called "β" is employed to facilitate the interpretation of the performance map by the computer. Afterwards, the produced power in the turbine is then calculated based on the enthalpy drop through the turbine.

Ducts: The recirculation path, intake and exhaust of the gas turbine are treated as adiabatic ducts with pressure loss. In off-design conditions, the pressure loss varies due to changes in the mass flow rate and thermodynamic conditions. Equation (9) presents a model that accounts for the deviation in the pressure loss factor during off-design conditions based on corrected mass flow rates ($\dot{m}_c$).

$$F = F_{dp} \left[\frac{\dot{m}_c}{\dot{m}_{c,dp}} \right]^2 \tag{9}$$

Gas turbine: Knowing the thermodynamic state of the gas in the inter component stations, gas turbine performance is determined based on a Brayton cycle. Shaft power delivered, fuel consumption, thermal efficiency, and CO_2 emission per MWhr are calculated according to equations (10)–(14).

$$P_{GT} = \eta_{mech} \left[P_{turb} - \frac{P_{comp}}{\eta_{mech}} \right] \quad single \; spool \; gas \; turbine \tag{10}$$

$$P_{GT} = \eta_{mech} P_{LP,turb} \quad two \; spool \; gas \; turbine \tag{11}$$

$$\dot{m}_f = \phi \dot{m}_{air} \tag{12}$$

$$\eta_{th} = \frac{P_{GT}}{\dot{m}_f FHV} \tag{13}$$

$$CO_{2,MWhr} = \frac{36 \times 10^8 n(\dot{m}_{CO_2,out} - \dot{m}_{CO_2,in})}{n P_{GT} + P_{ST}} \tag{14}$$

Heat exchangers: Under reduced load conditions, the heat transfer and pressure loss in heat exchangers deviate from their design values due to changes in flow conditions. To simulate the heat recovery system and steam condenser in off-design conditions, a generic heat exchanger model described in [54] is utilized here. The pressure loss in a heat exchanger is determined by considering the variations in the friction factor, mass flow rate, and density, as stated in equation (15). The suggested method in [55] is employed to assess the friction factor of generic heat exchangers under off-design conditions, as shown in equation (16).

$$\frac{\Delta P}{\Delta P_{dp}} = \left(\frac{f}{f_{dp}} \right) \left(\frac{\dot{m}}{\dot{m}_{dp}} \right)^2 \left(\frac{\rho}{\rho_{dp}} \right)^{-1} \tag{15}$$

$$\frac{1}{\sqrt{f}} = -1.8 log_{10} \left[\left(\frac{\epsilon_D}{3.7} \right)^{1.11} + \frac{6.9}{Re_D} \right] \tag{16}$$

The calculation of outlet temperatures in heat exchangers relies on the model introduced in [56]. This method employs the heat exchanger effectiveness and heat transfer coefficient, as depicted in equation (17). In [54], a general modelling approach is proposed to estimate the

variation in the heat transfer coefficient under off-design conditions, as represented by equations (18) and (19). The model utilizes the Nusselt number and thermal diffusivity of the fluid to evaluate heat transfer. Simulating the once-through boiler poses a difficulty due to the transition of water thermodynamic phase from subcooled state to superheated steam. Consequently, determining the precise temperature and the exact moment when this phase transition occurs becomes crucial. To address this, an iterative method is employed to calculate the specific point at which the phase change initiates.

$$\frac{\Delta T_S}{\Delta T_L} = \exp \left[-\frac{UA}{C_{min}} \left(1 - \frac{C_{min}}{C_{max}} \right) \right]$$

$$C_{min} = \min[C_{cold}, C_{hot}] \quad and \quad C_{max} = \max[C_{cold}, C_{hot}]$$

$$\Delta T_S = \min \left[(T_{hot,out} - T_{cold,in}), (T_{hot,in} - T_{cold,out}) \right]$$

$$\Delta T_L = \max \left[(T_{hot,out} - T_{cold,in}), (T_{hot,in} - T_{cold,out}) \right] \tag{17}$$

$$\frac{U}{U_{dp}} = \frac{2 \bar{\beta}_{cold} \bar{\beta}_{hot}}{\bar{\beta}_{cold} + \bar{\beta}_{hot}} \tag{18}$$

$$\bar{\beta} = \left(\frac{Nu}{Nu_{dp}} \right) \left(\frac{k}{k_{dp}} \right) \tag{19}$$

Steam turbine: An axial turbine configuration is chosen for the purpose of expanding superheated steam and generating power. While many previous studies utilized Stodola's "cone law" to predict the swallowing capacity of steam turbines, Beckmann's method has demonstrated superior accuracy, especially for highly loaded turbines or the turbines with choked stages [57]. In this study, the Beckmann method presented in [58] is employed to determine the swallowing capacity of the steam turbine at various pressure ratios. A generic steam turbine performance map is developed based on the Beckmann methodology and represented in the Fig. 3. The expansion ratio is normalized with respect to the critical expansion ratio, which represents the maximum expansion ratio the turbine can handle before experiencing choking. Similarly, the corrected mass flow rate is normalized based on the maximum swallowing capacity of the turbine.

The *Parson* number is suggested in [59] to estimate the efficiency of a steam turbine under part-load operating conditions. Fig. 4 illustrates the model used for steam turbine efficiency based on the relative *Parson* number. The relative *Parson* number is calculated based on relative isentropic enthalpy drop in the turbine (equation (20). In certain scenarios, a portion of the turbine experiences wet expansion, resulting in a mixture of water and steam exiting the turbine. *Baumann* [60] proposed a corrective model to consider the effects of wet expansion in the steam turbine. To identify the saturation, point at which wet expansion
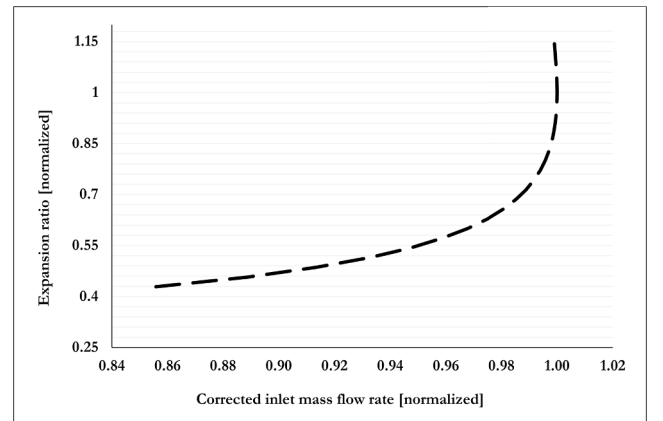

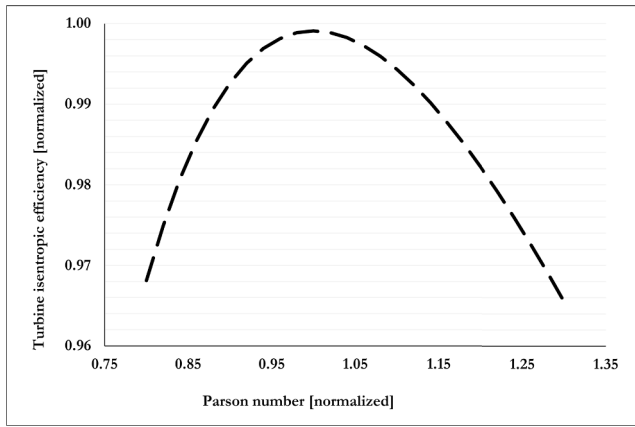**Fig. 3.** Steam turbine capacity.

Fig. 4. Steam turbine isentropic efficiency map.

commences, an iterative procedure is employed. While the dry expansion segment does not require correction, the isentropic efficiency of the turbine is adjusted in the wet expansion section using equation (21). Although the *Baumann* factor (α) varies depending on the average steam wetness [61], a constant value of 0.7 is assumed to be sufficiently accurate when modelling steam turbines with a weighted mean steam wetness between 0.005 and 0.025.

$$\frac{X}{X_{dp}} = \frac{\Delta H_{s,dp}}{\Delta H_s} \tag{20}$$

$$\eta_{wet} = \eta_{dry}(1 - \alpha y_{mean}) \tag{21}$$

Pump: A variable speed pump is utilized to pressurize the water in the steam cycle. This variable speed pump offers the ability to achieve the desired pressure increase for different rates of water flow. To predict the performance of the pumps in power plant applications, a method described in Reference [62] is used and expanded to incorporate variable frequency drive pumps, as proposed in Reference [63]. A comprehensive chart, depicted in Fig. 5, is created to assess the pump's increase in head pressure and its isentropic efficiency based on the mass flow rate and relative speed.

2.3. Off design performance

An algorithmic framework and computer solver have been developed to assess the operational performance of the combined cycle system across a range of operating conditions, as depicted in Fig. 6. The system's performance may deviate from its design parameters due to
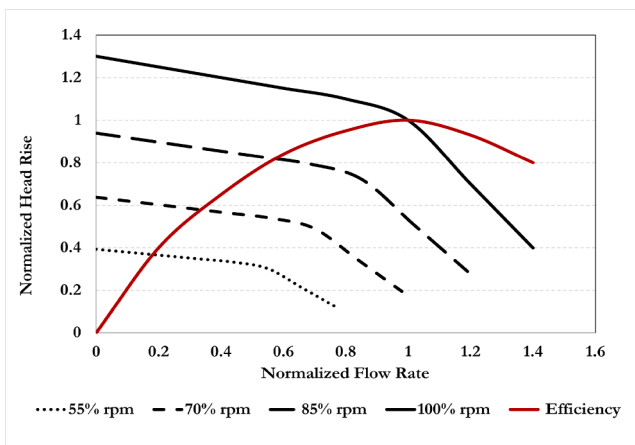
Fig. 5. Variable speed pump performance.
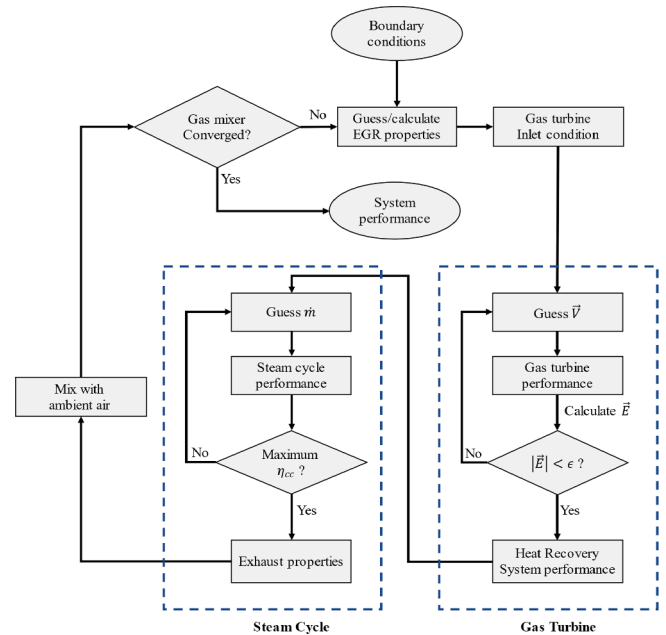
Fig. 6. Off-design solver logic flow chart.

factors such as fluctuations in load demands, ambient conditions, variations in fuel composition, or other relevant factors. The solver identifies control configurations that can yield the desired performance or align with the prescribed boundary conditions of the combined cycle. Subsequently, key performance indicators of the cycle are evaluated to provide a precise and accurate assessment of the overall system performance.

Initially, the solver conducts an analysis of the gas turbine to assess the flow characteristics at different stations along the gas turbine. By obtaining the relevant properties of the gas discharged from the turbine, the inlet conditions to the bottoming cycle are determined. Afterwards, the solver search and finds an optimum operating option for the steam cycle to match with the input from the topping cycle. A sliding pressure control strategy is used and optimized for maximum combined cycle thermal efficiency. Various water mass flow rates are estimated and tested to identify the optimal value that yields the highest combined cycle efficiency. A comprehensive explanation of the technique utilized to determine the optimal off-design operation point of the steam cycle is discussed in reference [16]. A fraction of the exhaust flow is recirculated and mixed with the inlet air of the gas turbine. Considering that this process alters the composition and temperature of the inlet air, the solver iteratively converges on the properties of the mixed air, ensuring a consistent performance evaluation.

The assessment of gas turbine performance under off-design conditions is conducted using a method proposed in reference [52]. This method employs an iterative solving approach, where a vector of iterative variables ($\vec{V}$) is initially estimated and subsequently updated until convergence is achieved in the convergence criteria vector ($\vec{E}$). The convergence vector, also referred to as the matching vector, characterizes the conditions at which the boundary conditions of the gas turbine components are matched. The vector elements of iterative variables ($\vec{V}$) and matching criteria ($\vec{E}$) are defined in Table 2 for single-spool and two-spool gas turbines.

The enhancement of system performance is primarily assessed through the measurement of combined cycle efficiency, which serves as the key indicator. Equation (22) provides the definition of combined cycle efficiency used here for a system comprising n gas turbine units and a single pressure level steam bottoming cycle. The fuel heating value (FHV) used in this formulation is the lower heat value associate with the

Table 2

Gas turbine off-design solver parameters.

single-spool gas turbine		two-spool gas turbine	
$\vec{V}$	$\vec{E}$	$\vec{V}$	$\vec{E}$
TIT*	$P_{GT} - P_{demand}$	TIT*	$P_{comp}/\eta_{mech} - P_{turb}$
β_{comp}	$p_{GT,out} - p_{amb}$	β_{comp}	$p_{GT,out} - p_{amb}$
β_{turb}	$\dot{m}_{bur} - \dot{m}_{turb}$	$\beta_{turb,HP}$	$\dot{m}_{bur} - \dot{m}_{turb,HP}$
		$\beta_{turb,LP}$	$\dot{m}_{turb,HP} - \dot{m}_{turb,LP}$

* Turbine Inlet Temperature.

fuel.

$$\eta_{cc} = \frac{nP_{GT} + P_{ST}}{n\dot{m}_f FHV} \qquad (22)$$

2.4. EGR control strategy

One commonly employed method for controlling gas turbine load and exhaust gas temperature involves adjusting both fuel flow rate and inlet guide vanes. However, an alternative approach is to manipulate the ratio of recirculated warm gas instead of tuning the IGV. While closing the IGV decreases the gas turbine load by reducing air mass flow rate and pressure ratio, warm EGR achieves load reduction by increasing compressor power consumption due to higher inlet temperature. High inlet temperatures result in lower gas density within the compressor flow passage, thereby reducing the aerodynamic throat area between compressor vanes while the original passage geometry is fixed. This approach presents a potentially more efficient means of controlling

pressure and mass flow rate within the compressor. From a systematic standpoint, the corrected speed and corrected mass flow rate of the compressor are shifted in high inlet temperatures. Therefore, the mass flow rate and pressure ratio would decrease without closing the IGV.

In each off-design operating condition, EGR ratio is manipulated to achieve the desired gas turbine load, while the inlet guide vanes remain unchanged. However, there are certain limitations that determine the range of viable options for selecting the EGR ratio. Technological constraints related to the materials used in turbine blades, supporting casings, and inlet filtration systems impose limits on the allowable temperature range of the working fluid at different stages. The turbine inlet temperature and exhaust gas temperature are confined to the design values of the gas turbine, considering the current level of technology. The maximum allowable compressor discharge temperature and compressor inlet temperature are being increased to approximately 550 °C and 115 °C, respectively. These temperature increments which are around 50 °C, appear to be achievable based on the technological advancement trend. In addition to temperature restrictions, the surge margin of the gas turbine is closely monitored to ensure it remains within an acceptable range, typically higher than 10%.
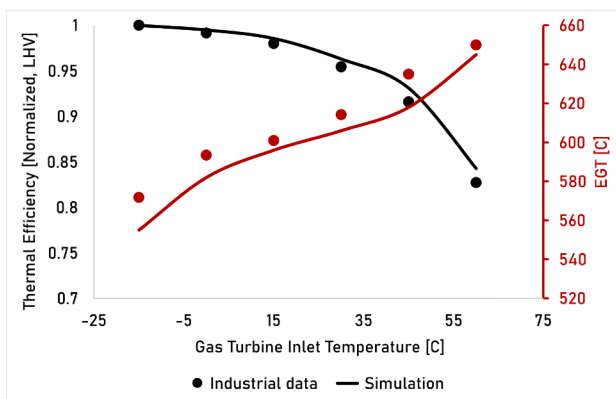
2.5. Verification

The models presented in this study have been implemented as a digital design and simulation tool using MATLAB [64]. This in-house simulation tool, called CCsim, incorporates a graphical user interface that allows users to analyze novel strategies in decarbonized gas turbine combined cycles. This in-house tool is primarily developed for the
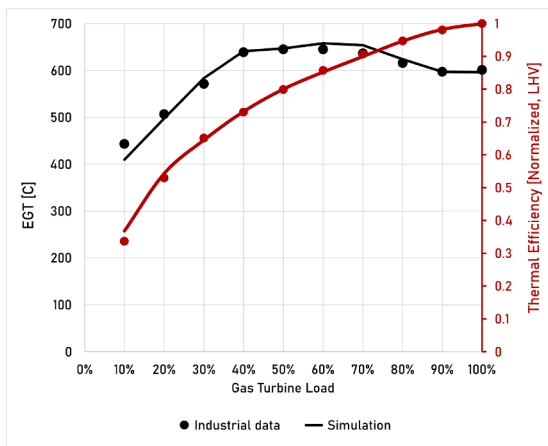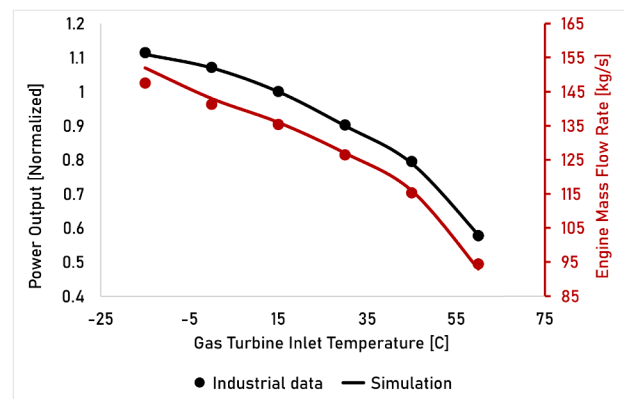

(a) part-load operation
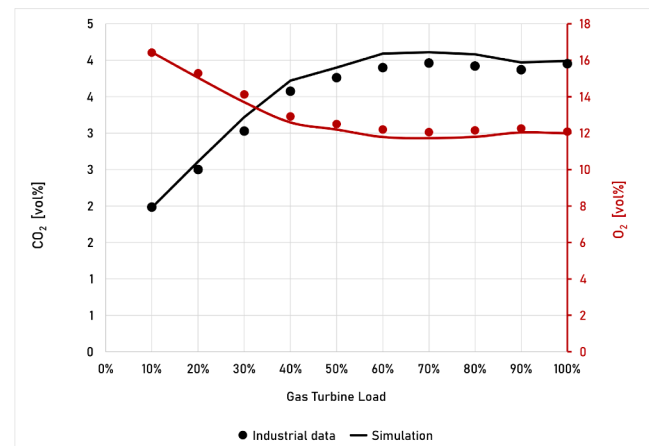
(b) discharge mixture composition

(c) ambient temperature variation

(d) ambient temperature variation

Fig. 7. Single-spool gas turbine performance verification.

purposes of this study and has been verified using industrial data and information from the open literature.

The validation process for the single-spool gas turbine model involved comparing it with a Siemens in-house performance model of an SGT-800 gas turbine provided by the manufacturer. The results of this comparison, demonstrate a good correlation between the model and the industrial data, in the range of 10% to 100% gas turbine load. Fig. 7(a) shows that the gas turbine's EGT and thermal efficiency are well correlated with the industrial data. To further enhance confidence in the accuracy of the model's predictions regarding emissions and gas composition, the discharge CO_2 and O_2 content were examined and verified for the Siemens SGT-800 case across the 10% to 100% gas turbine load range, as depicted in Fig. 7(b).

The utilization of warm exhaust gas recirculation in gas turbine operation leads to an elevation in the inlet temperature. Consequently, the gas turbine model was subjected to verification using industrial data specifically for high inlet temperature operation. Fig. 7(c) provides confirmation of the model through the comparison of power output and engine mass flow rate as the ambient temperature varies from −15 to 60°Celsius. Similarly, Fig. 7(d) serves as a verification of the model by examining the exhaust gas temperature and thermal efficiency within the range of inlet temperatures.

The validation of the gas turbine model includes two-spool configurations, where the model results are compared with the performance data of the Siemens SGT-750 gas turbine. The performance data used for comparison is sourced from GT MASTER 29 [65], a dependable performance library for gas turbines. As shown in Fig. 8(a), the model results are in good agreement with the reference data within the gas turbine load range of 30% to 100%.

Once the gas turbine model has been validated, the verification process extends to the steam cycle and the overall combined cycle model. To achieve this, a study referenced as [24], which specifically examines the operation of a combined cycle with EGR during part-load conditions, is selected for verification purposes. The study focuses on enhancing the part-load operation of two SGT-800-50 gas turbines and a single pressure level steam bottoming cycle by utilizing warm EGR. Fig. 8(b) illustrates the excellent agreement between the outcomes generated by the developed modeling tool and the data provided in [24].

2.6. Case studies

Two case studies have been conducted to assess the proposed operational strategy, taking into consideration that the characteristics and behaviors of single-spool gas turbines and two-spool gas turbines are distinct. A combined cycle power plants is designed for assessment of each case. To evaluate each case, a combined cycle power plant has been designed. In this design, a Siemens SGT-800 single-spool gas turbine and a Siemens SGT-750 two-spool gas turbine have been chosen to function as the topping cycle in the case studies. In each case, the combined cycle configuration consists of two parallel operating gas turbine units, along with a steam bottoming cycle. The performance characteristics of the designed cycles at full load are presented in Table 3. The gas turbine units are operating under standard atmospheric conditions, which include a pressure of 1 atm, a temperature of 15 °C, and a relative humidity of 60%.

3. Results

This section presents an evaluation of the performance of the designed power plant under baseline conditions, serving as a reference case. Subsequently, the optimized operation incorporating warm EGR is assessed across a wide range of power outputs. The enhancements achieved in the part-load operation are quantified relative to the reference cases. Under the improved operation scenarios, an analysis is conducted on the key performance indicators to give an overview on the plant performance. To ensure the validity of the proposed operational strategy, technical limitations are thoroughly investigated. Additionally, various scenarios are discussed to provide a comprehensive overview of the potential performance improvements when employing warm EGR during part-load operation of combined cycles.

Table 3
Power plant performance at design point.

Parameter	Value	
	Single-spool gas turbine	Two-spool gas turbine
gas turbine units	2	2
steam turbine units	1	1
gas turbine power	61.5 MW	40 MW
steam cycle power	39.8 MW	9.6 MW
CO_2 emission	368 kg/MWhr	449 kg/MWhr
steam cycle efficiency	31.6 %	24.7 %
air mass flow rate	135 kg/s	115 kg/s
steam mass flow rate	36.5 kg/s	14.6 kg/s
air exhaust temperature	114 °C	263 °C
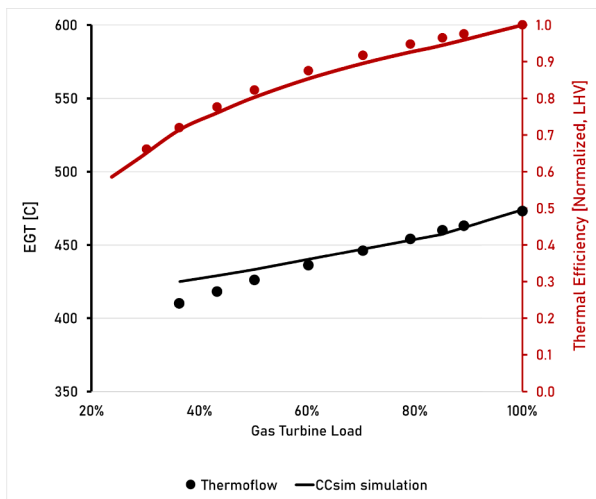
(a) two-spool gas turbine
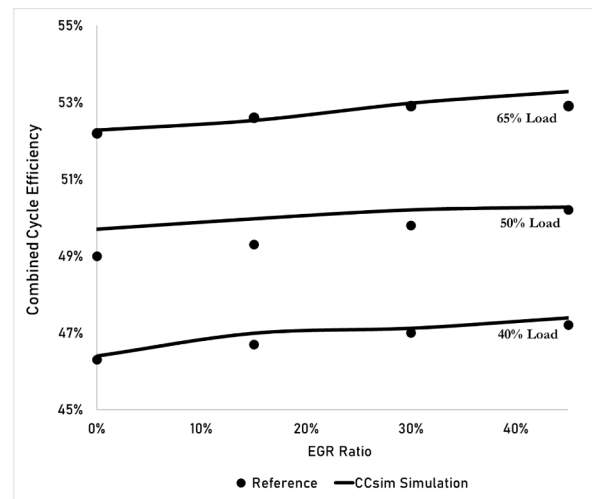
(b) combined cycle performance

Fig. 8. Digital tool verification.

3.1. One-spool gas turbine case

The performance of a combined cycle power plant with an SGT-800 gas turbine is analyzed under different load levels using the baseline operation strategy. In the baseline operation strategy, the IGVs are adjusted to control the overall performance of the cycle while the shaft speed is fixed. As the load request decreases, the baseline controller manipulates the IGVs to gradually increases the EGT while maintaining the Turbine Inlet Temperature (TIT) at the maximum level. When the plant load reaches 70% (equivalent to 60% gas turbine load), the EGT reaches its maximum allowable limit and remains constant until the gas turbine load decreases to 40%. For loads lower than 40%, both EGT and TIT decrease as the IGVs reach their most closed position. Fig. 9 illustrates the variations in EGT and TIT for the single-spool SGT-800 gas turbine during part-load operation, as controlled by the baseline control strategy. Fig. 10 presents a quantification of the decline in combined cycle efficiency throughout the load range. In the case of low loads, where the EGT is maintained at a high level, the efficiency of the bottoming cycle remains close to its designed value. However, the decline in gas turbine efficiency causes the combined cycle efficiency to decrease during part-load operation (as depicted in Fig. 10).

In the case of part-load operation, the implementation of a propped operation scenario with warm EGR has been found to enhance the combined cycle efficiency. This improvement is achieved while maintaining a similar TIT compared to the baseline operation (as demonstrated in Fig. 11). Conversely, this possibility has been identified to manipulate EGR ratio in a manner that the TIT is mitigated without adversely affecting system performance (as depicted in Fig. 12). This strategy effectively reduces thermal stress on turbine blades and increases the expected lifespan of the hot section components. Accordingly, it can be concluded that a range of operation scenarios exists that span from high efficiency strategies to improved life expectancy scenario.

An intermediate scenario has been selected to achieve a moderate increase in efficiency while also extending the operational lifespan of the gas turbine. This choice results in a 5-percentage-point enhancement in combined cycle efficiency, equivalent to a 20% relative increase in plant efficiency (as shown in Fig. 13). The improved performance contributes to reduced fuel consumption and a decrease in CO_2 emissions from the power plant. Fig. 14 demonstrates that at a 20% plant load, there is a reduction of 170 kg of CO_2 emitted to the environment per MWh of generated electricity. This represents a relative reduction of 37% in CO_2 emissions during part-load operation. Additionally, the recirculation of exhaust gas increases the CO_2 concentration in the flue gas as depicted in Fig. 14. This higher CO_2 concentration in the flue gas is advantageous for potential downstream carbon capture facilities. In addition to higher
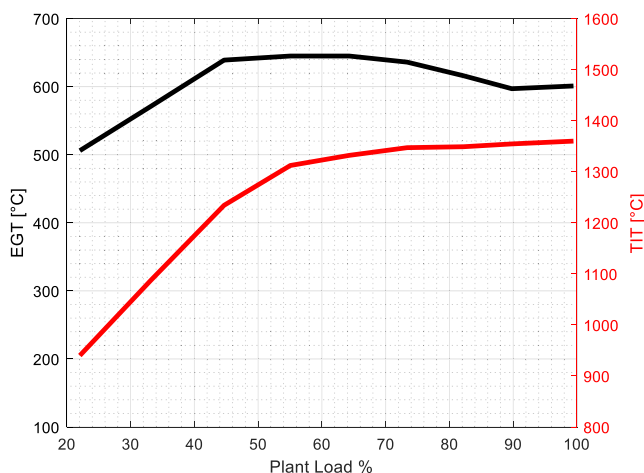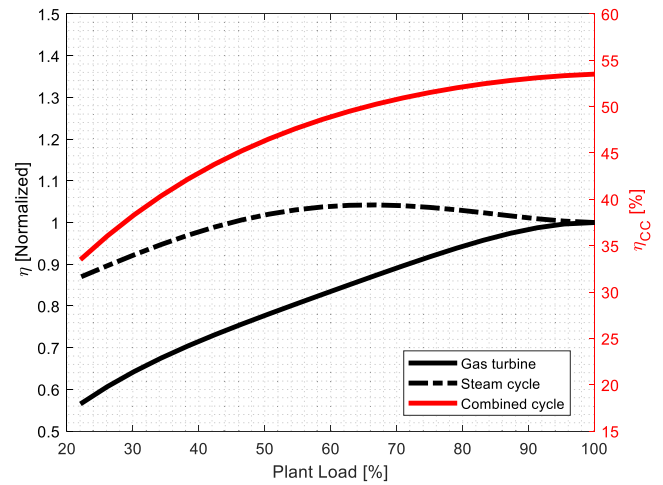
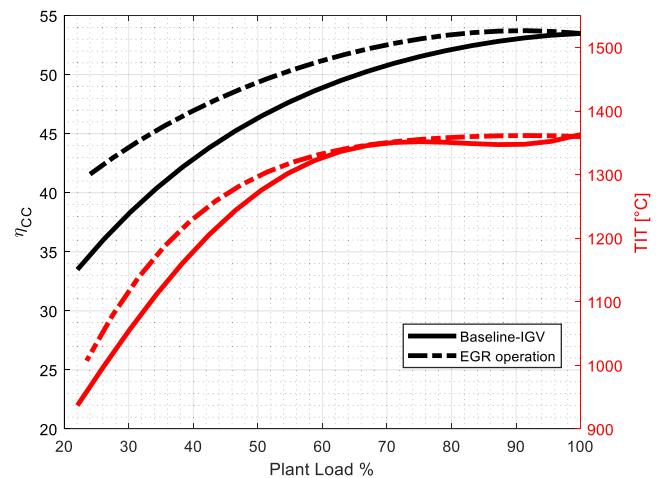**Fig. 10.** Baseline thermal efficiency (SGT-800).

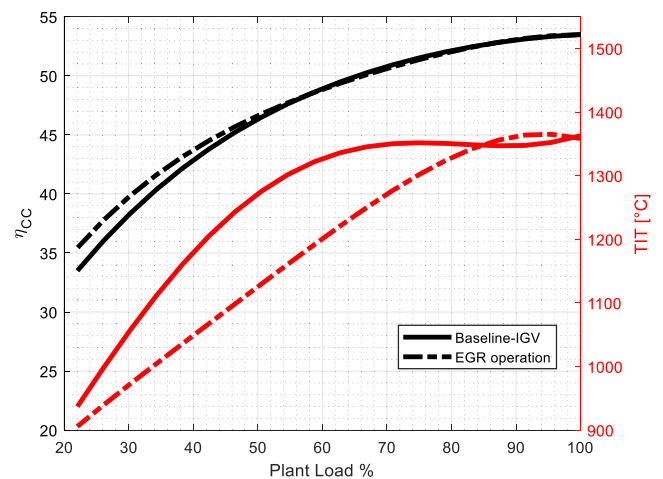**Fig. 11.** High efficiency enhancement scenario (SGT-800).

Fig. 12. Life expectancy enhancement scenario (SGT-800).

thermal efficiency, the other factor contributing to reducing specific CO_2 emission is that more power is extracted from the bottoming cycle for the same level of plant efficiency.

The manipulation of the EGR ratio is employed at different power output levels to regulate temperatures within the gas turbine sections.
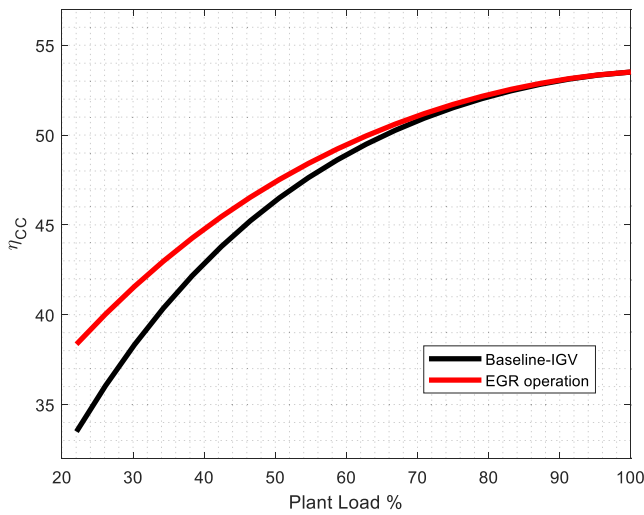
Fig. 9. Turbine temperatures at baseline operation (SGT-800).

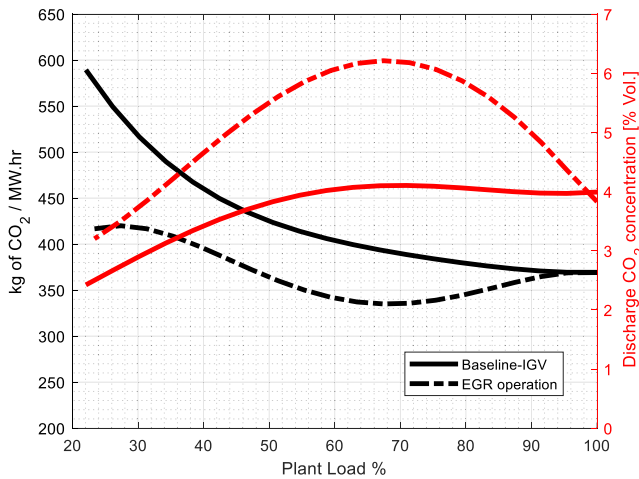**Fig. 13.** Part-load plant efficiency (SGT-800).

Fig. 14. Part-load CO_2 emission (SGT-800).

Notably, during part-load operation, a significant decrease of 60 °C is observed in both the TIT and EGT. This reduction contributes to a decrease in thermal stress experienced by the hot section components, as illustrated in Fig. 15. Furthermore, the temperatures at the compressor inlet 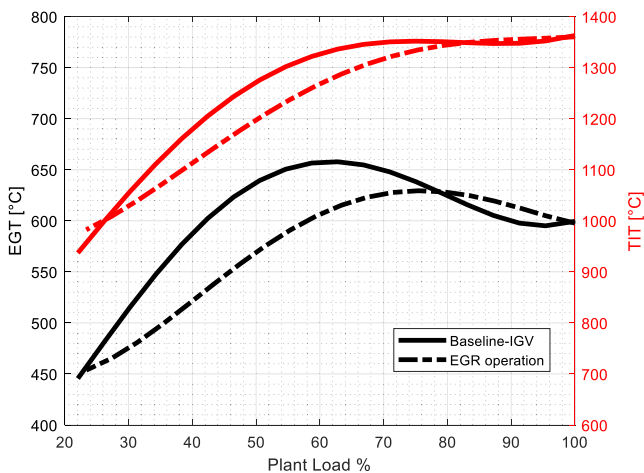and discharge are effectively maintained within the intended design limits, as depicted in Fig. 16. It is worth noting that the compressor temperatures surpass the design values due to the presence of warm gas recirculation within the cycle.

The proposed operational strategy involves a reduction in firing temperature, which subsequently leads to a decrease in burner loading across the operational range. This reduction in firing temperature results in more efficient combustion at the burner, as demonstrated in Fig. 17. Increased combustion efficiency contributes to decreasing fuel consumption for a given amount of heat released in the burner. However, there is a concern regarding the recirculation of oxygen-depleted air into the cycle, as it may impact the completeness of combustion due to insufficient oxygen in the unburnt air. To address this, the concentration of O_2 in the combustor discharge is calculated to ensure complete combustion in the presence of warm gas recirculation. Fig. 18 indicates that an acceptable amount of oxygen remains in the burnt gas, suggesting that gas recirculation can be implemented while maintaining complete combustion within the system. It is essential to highlight that the oxygen concentration at the gas turbine inlet is identical to the oxygen concentration before combustion. This uniformity is maintained because the oxygen concentration remains constant from the gas turbine inlet to the entrance of the combustion chamber, as depicted in Fig. 18.

The results demonstrate that the gas turbine efficiency is higher when employing the proposed EGR operation strategy at reduced loads compared to the baseline IGV control strategy. Fig. 19 illustrates that the gas turbine efficiency is slightly improved with the proposed operational strategy, despite the steam cycle efficiency remaining unchanged. It is important to note that the steam cycle maintains the same level or slightly decreased as the baseline operation, primarily due to the unchanged Exhaust/decreased EGT in the proposed scenario. Furthermore, Fig. 20 indicates that the power distribution between the gas turbine units and the steam cycle remains almost unchanged when transitioning from baseline IGV operation to the warm EGR operation during part-load conditions. The EGR ratio corresponded to the designed control strategy of single spool gas turbine is illustrated in Fig. 21. The EGR ratio is increased as the plant load is reduced from 100% to 75%. Beyond this range, EGR is limited to 50% to accommodate the limitations regarding temperatures in the gas turbine.

The comparative analysis reveals that load regulation utilizing warm EGR is more effective than regulation using variable IGV in terms of compressor efficiency, as depicted in Fig. 21. In IGV operation scenario, controller adjusts the compressor vanes to decrease the geometric area, thereby reducing compressor capacity. On the other hand, the warm EGR controller achieves a reduction in aerodynamic area by introducing warm air into the compressor. This reduces the density and consequently, the mass flow rate capacity through the blades passage. Investigations indicate that the latter approach is a more efficient method
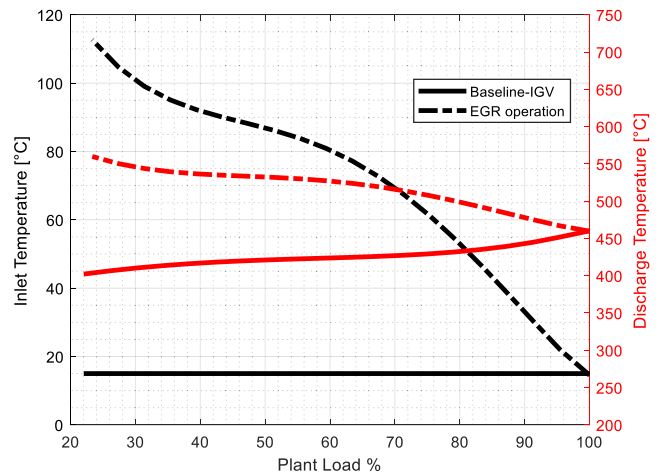

Fig. 15. Part-load turbine temperatures (SGT-800).

Fig. 16. Part-load compressor temperatures (SGT-800).
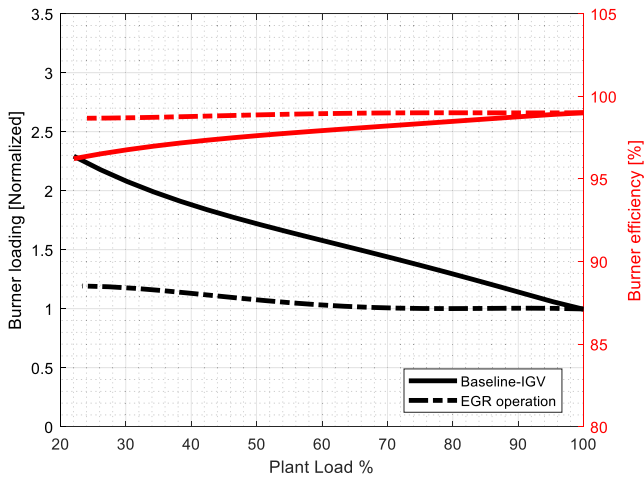
Fig. 17. Part-load burner performance (SGT-800).
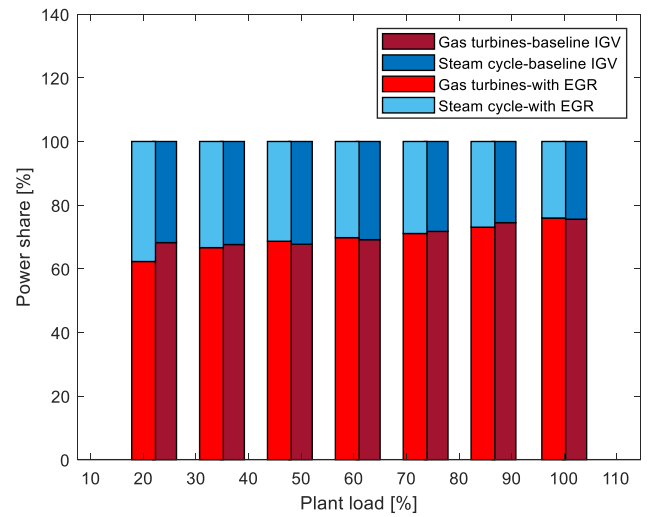

Fig. 20. Combined cycle power distribution (SGT-800).
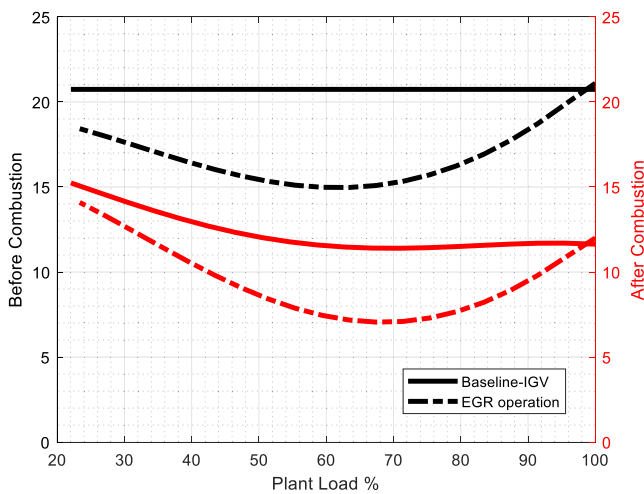

Fig. 18. Part-load gas composition (SGT-800).
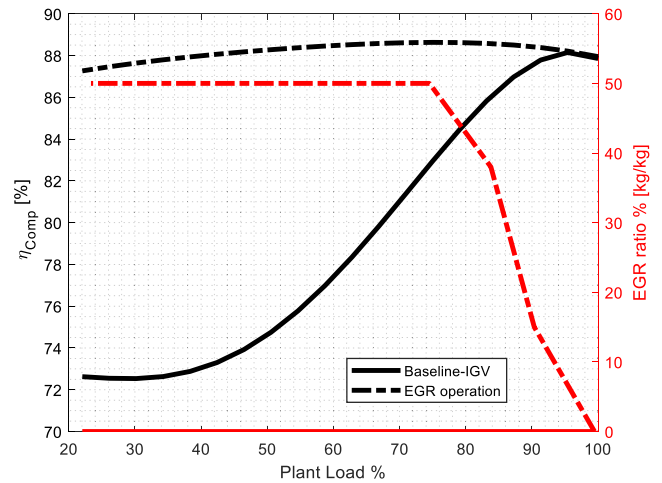

Fig. 21. Simulated compressor efficiency and EGR ratio (SGT-800).
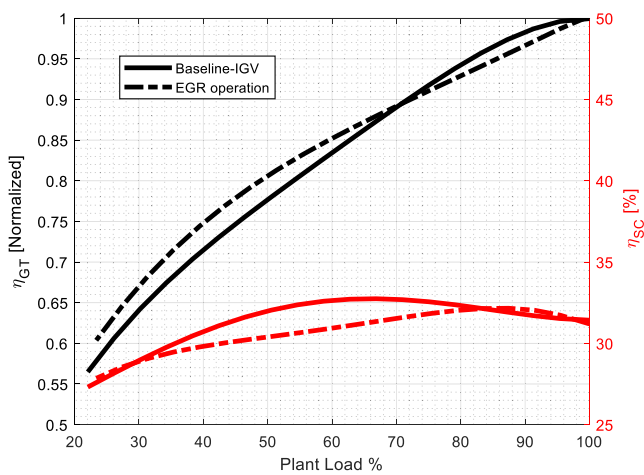

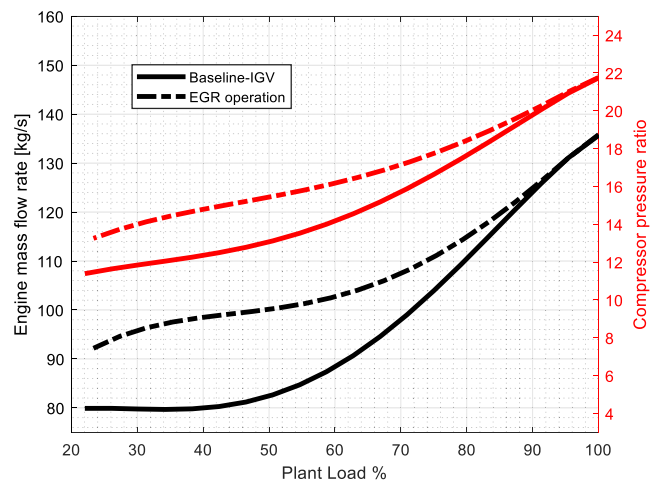**Fig. 19.** Part-load thermal efficiencies (SGT-800).

Fig. 22. Part-load engine performance (SGT-800).

for regulating compressor capacity in single-spool gas turbines, as shown in Fig. 21. By enhancing compression efficiency, the available compressor power can be used for higher mass flow rates and higher pressure-ratios compared to baseline case (Fig. 22). The improved compressor efficiency and increased pressure ratio contribute to a more

efficient overall gas turbine operation.

3.2. Two-spool gas turbine case

A comprehensive performance analysis of the power plant featuring the SGT-750 gas turbine is conducted under baseline operating conditions. In the baseline operation of the two-spool gas turbine case study, there is no gas recirculation, and variable geometry vanes are not employed. Instead, the gas turbine shaft speed gradually decreases during part-load conditions. The baseline performance analysis reveals an expected decrease in the efficiency of the combined cycle during reduced load operation. One of the primary factors contributing to this efficiency decay is the reduction in gas turbine EGT during part-load operation, which consequently limits the evaporation temperature in the bottoming cycle (refer to Fig. 23). Consequently, the heat available to the steam cycle during part-load operation exhibits lower quality, indicated by a lower temperature. Fig. 24 provides an illustrative representation of the decline in steam cycle efficiency and power at part-loads, attributable to the reduced availability of heat with lower quality.

The Fig. 25 depicts the illustration of improving the combined cycle efficiency in a two-spool gas turbine scenario through the recirculation of warm gas. This technique leads to enhanced performance across various power output levels. At a plant load of 30%, the combined cycle efficiency exhibits a notable increase of 4 percentage points. This improvement corresponds to a relative enhancement of approximately 14% in the overall cycle performance, offering significant potential for reducing fuel consumption in decarbonized plants or achieving emission reduction in natural gas combined cycles.

The calculation of CO_2 emission reduction is performed during part-load operation using the proposed warm EGR scenario. Fig. 26 illustrates a significant reduction of 150 kg of CO_2 emissions for every MWhr of energy generated at a plant load of 30%. This reduction corresponds to a relative carbon emission decrease of approximately 21% from the entire plant, thereby promoting environmentally friendly operations and alleviating the carbon tax burden for the operator. Additionally, the CO_2 volumetric concentration exiting the cycle doubles from 2.5% to 5% at 30% plant load, which presents a favorable condition for potential carbon capture facilities downstream of the power plant.

Fig. 27 presents the graphical representation of the optimized control setting for the EGR ratio in the improved scenario across the operational load range. The EGR ratio value is fine-tuned to maintain temperatures close to the design values during part-load operation. However, it is important to note that the maximum ratio of recirculation is constrained to 50% due to the temperature constraints at both the compressor inlet and compressor discharge (as illustrated in Fig. 28). Based on Fig. 27, the EGR ratio exhibits a gradual increase as the power demand
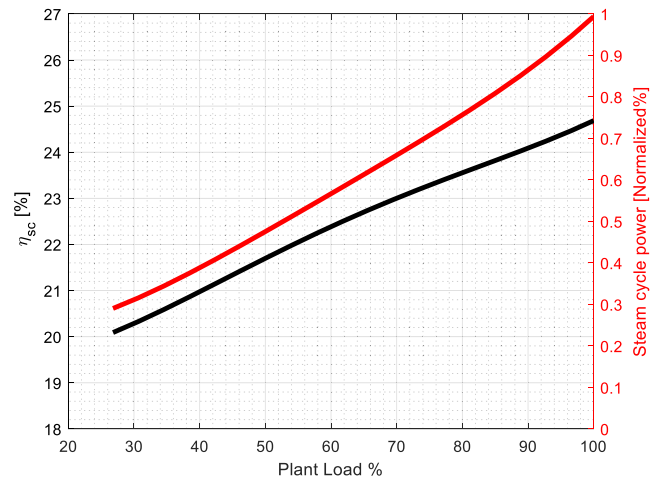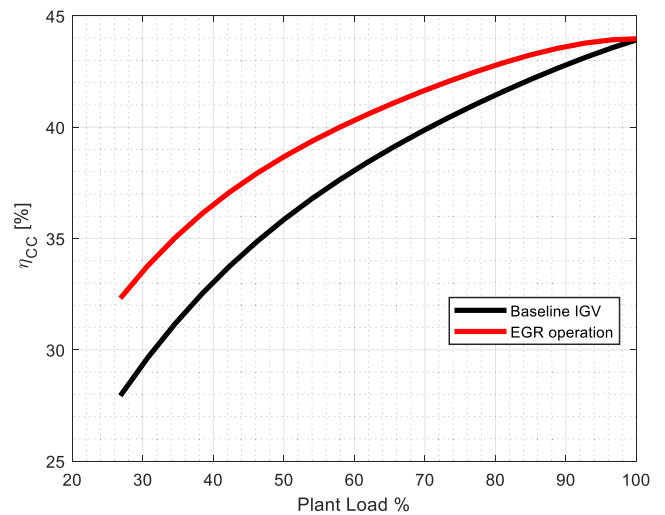

Fig. 24. Steam cycle part-load performance.

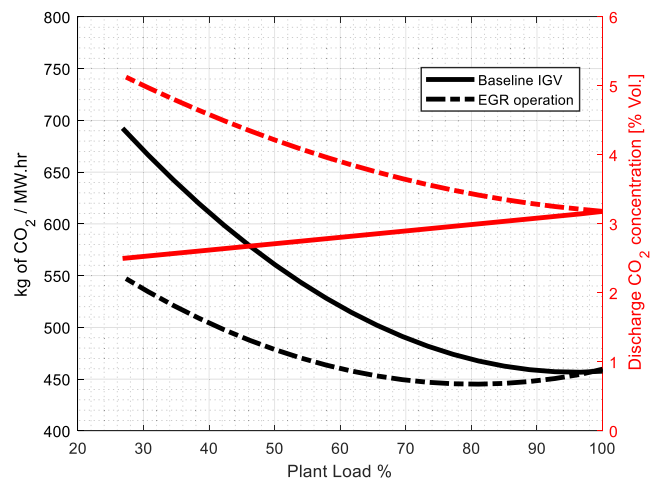**Fig. 25.** Plant efficiency improvement (SGT-750).

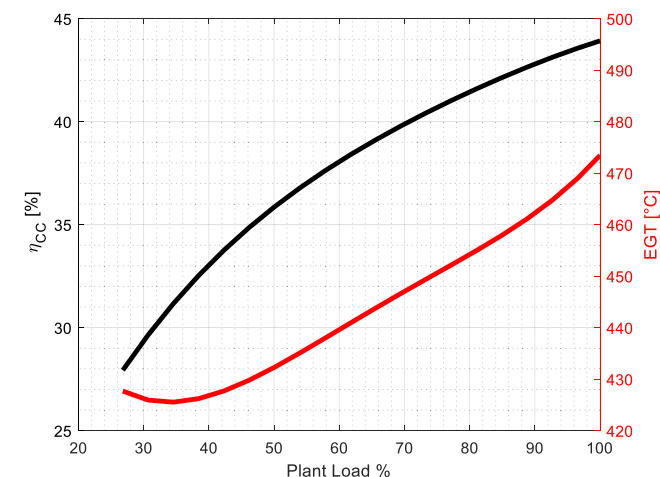**Fig. 26.** Plant CO_2 emission reduction (SGT-750).

Fig. 23. SGT-750 baseline operation.

decreases, serving the purpose of regulating the power output from the plant. It is observed that when a higher EGR ratio is introduced to the engine, the compressor inlet temperature experiences an elevation. This pattern persists until the plant load reaches 40%, at which point the
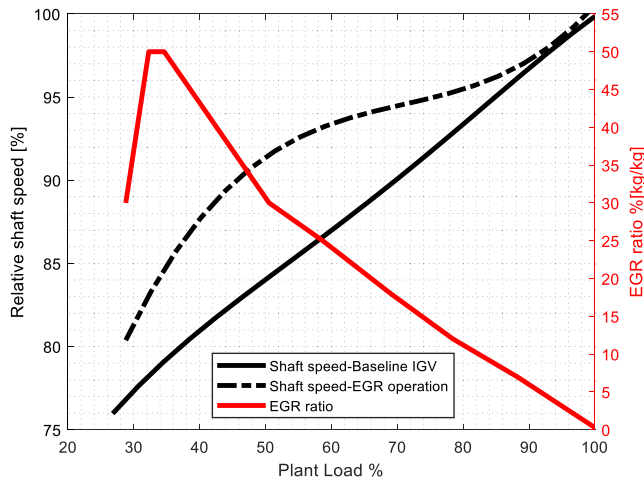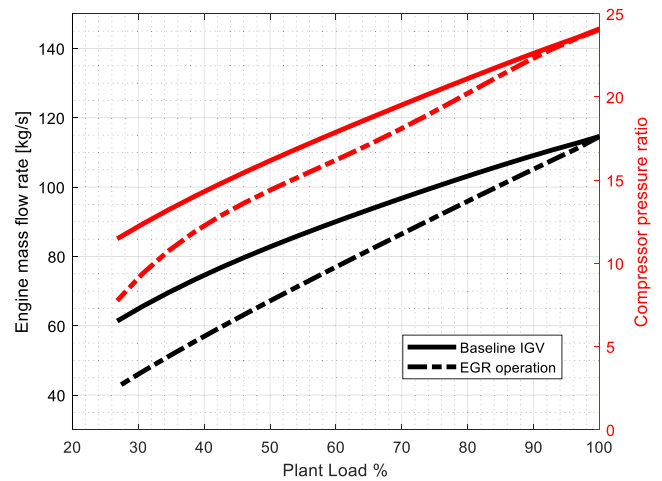
Fig. 27. Part-load control settings (SGT-750).

Fig. 29. Part-load engine performance (SGT-750).
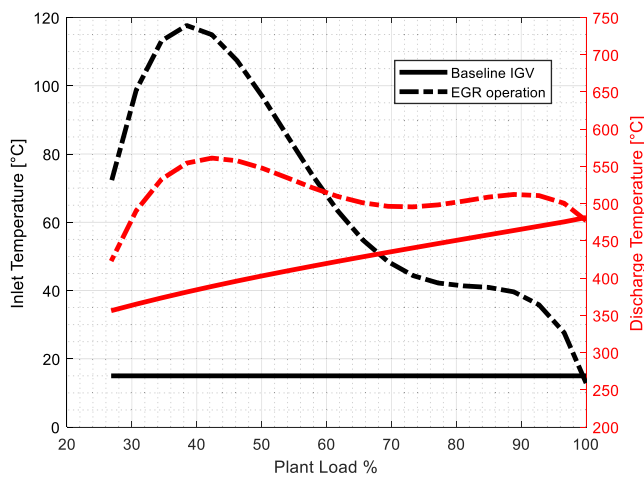

Fig. 28. Part load compressor temperatures (SGT-750).
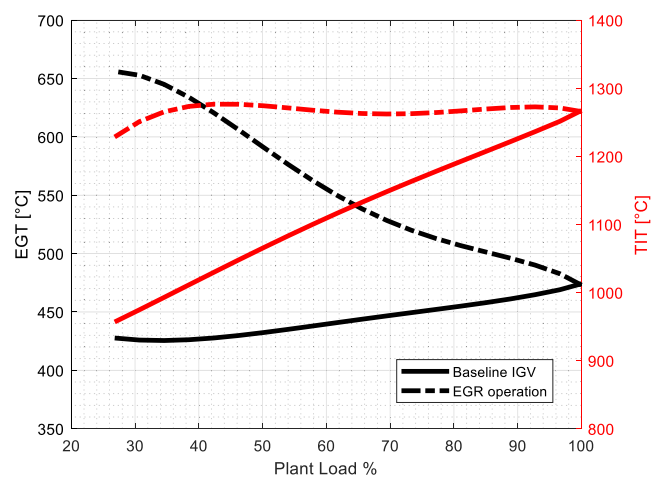

Fig. 30. Part-load turbine temperatures (SGT-750).

compressor inlet temperature reaches its maximum threshold in conjunction with a 50% EGR ratio.

For power loads below 40%, the maximum acceptable EGR ratio undergoes a reduction and remains below 50%. This limitation is imposed by the lower boundary set by the operational mass flow rate range of the low-pressure turbine. In this case, the low-pressure turbine operates at its minimum capacity due to the decreased load magnitude. In the EGR operation scenario, the IGV setting remains unchanged and fully open, while the gas generator speed is reduced relative to design value during part-load conditions. The part-load shaft speed is higher compared to the baseline IGV operation to account for the lower gas density and pressure with reduced engine mass flow rate in the gas turbine (as depicted in Fig. 29).

By adjusting the EGR ratio, the exhaust temperature of the gas turbine is increased during part-load operation, thereby providing higher-quality heat to the steam cycle. Fig. 30 illustrates the rise in EGT and turbine inlet temperature during part-loads. The proposed EGR operation strategy effectively maintains the turbine inlet temperature close to the designed value, resulting in improved combustion efficiency in the gas turbine due to reduced burner loading. This is depicted in Fig. 31, which showcases an almost flat efficiency curve for the burner, indicating reduced loading for load ranges exceeding 40%. Lower burner loading enables the combustor to achieve reduced fuel consumption and lower emissions under the same thermofluidic conditions. The measure of burner loading serves as an indicator of the extent to which the combustion process has time for an efficient heat release.

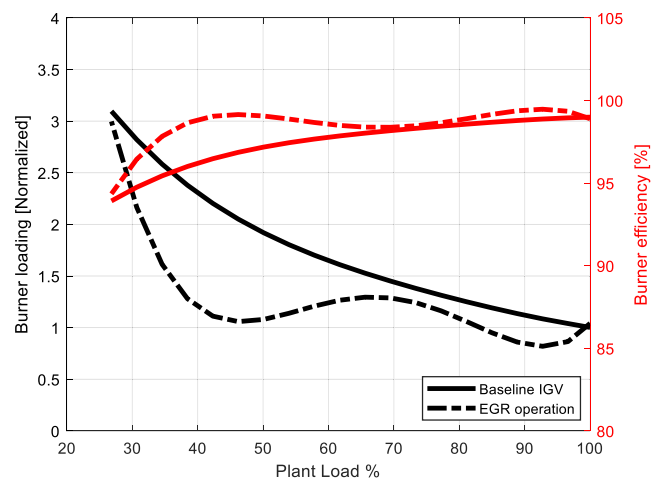**Fig. 31.** Part-load burner performance (SGT-750).

The combustor discharge is analyzed to determine the level of oxygen (O_2) concentration present, ensuring that combustion is fully achieved even when low oxygen content gas is being recirculated. Based on Fig. 32, it is observed that there is enough oxygen remaining in the burned gas, indicating that the implementation of gas recirculation can
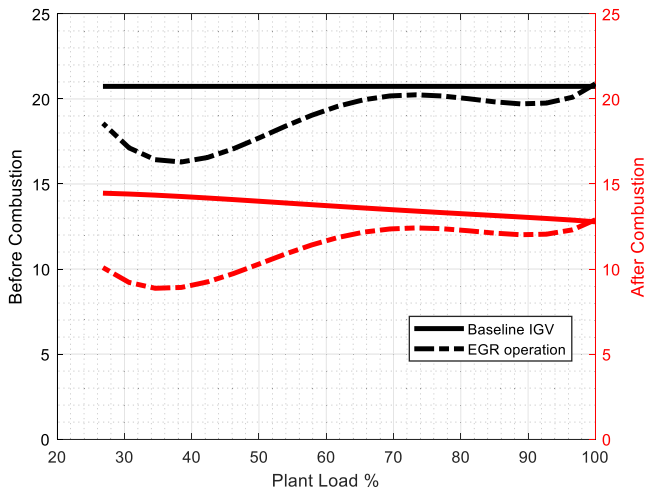
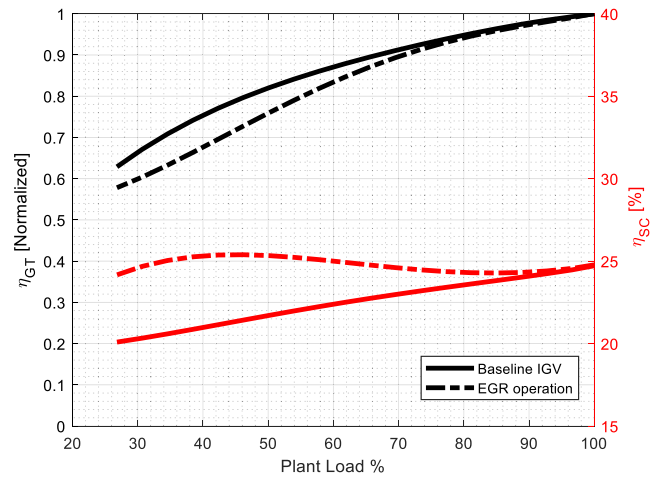**Fig. 32.** Oxygen concentration [%vol] (SGT-750).

Fig. 34. Part load thermal efficiency (SGT-750).

be carried out without compromising the completeness of combustion in the system.

By supplying a higher temperature heat source to the bottoming cycle, a larger proportion of the total power generation is allocated to the steam cycle compared to the gas turbines. Fig. 33 depicts the distribution of power generation between the steam cycle and gas turbine units for the two operation strategies. The implementation of warm gas recirculation as a load management strategy enables the bottoming cycle to generate more power, which experiencing a lesser decline in efficiency during part-loads compared to the gas turbines. This is evident from Fig. 34, which demonstrates that the thermal efficiency of the steam cycle remains relatively constant with the warm EGR scenario, whereas the gas turbines exhibit a decrease in efficiency during part-load conditions.

It is important to make a remark when considering the utilization of the SGT-750 two-spool gas turbine as the topping cycle. While the performance at part-load conditions is improved, it is worth noting that the efficiency at the design point and full load is relatively low, as indicated in Table 3. This can be attributed to the fact that the SGT-750 exhibits a lower EGT of approximately 470 °C, in contrast to the SGT-800's EGT of around 600 °C. Based on this observation, it can be concluded that two-spool gas turbines with lower EGT values suffer from the disadvantage of limited potential for the bottoming cycle.
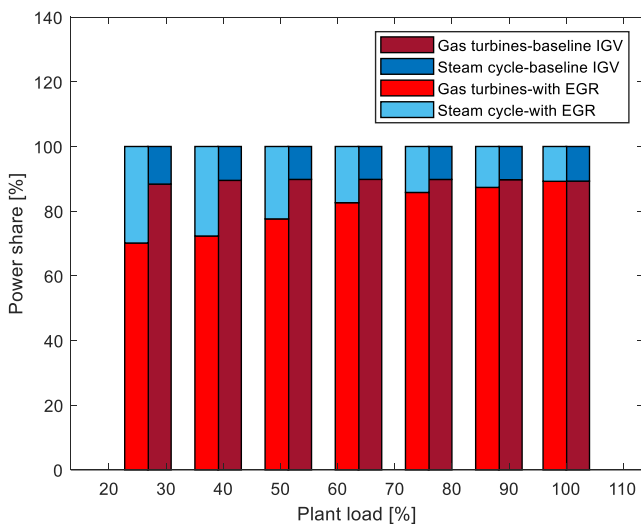
4. Conclusion

This article proposed a solution to enhance the part-load thermal efficiency of gas turbine combined cycles used for offshore power generation. The proposed solution involves the implementation of warm exhaust gas recirculation in the gas turbine cycle, a method that has been studied by researchers and engineers for its benefits in carbon-free combustion and carbon capture mechanisms. The suggested operation strategy is evaluated for both single-spool and two-spool gas turbines, operating in conjunction with a steam bottoming cycle extracting power from the gas turbines waste heat. However, further investigations and test on different machines in different scenarios can boost the reliability in the proposed method and tool. The main advantages of this strategy include higher power plant efficiency, less fuel consumption, less CO_2 emission, and higher life expectancy for the equipment. The article also presented an in-house design and simulation tool that allows for the evaluation of gas turbines equipped with modern gas recirculating systems and flexibility in operation with carbon-free fuel mixtures. The tool was successfully verified with industrial data and data available in the open literature. Through quantified measurements, the article demonstrated the improvements in efficiency boost, emission reduction, and fuel consumption achieved with the proposed solution.

The study's findings demonstrated 20% and 14% efficiency boost in part-loads for single-spool and two-spool gas turbine cases, respectively. The study showed a 37% and 21% reduction in specific CO_2 emission for single-spool and two-spool gas turbine cases, respectively. 50 °C turbine inlet temperature reduction was offered in the single-spool gas turbine case to extend the lifespan expected from the gas turbine. The article introduced the concept of warm exhaust gas recirculation as a solution to enhance part-load thermal efficiency and reduce environmental impact in the combined cycle power plants.

CRediT authorship contribution statement

Mohammad Ali Motamed: Conceptualization, Formal analysis, Methodology, Software, Writing – original draft, Writing – review & editing. **Magnus Genrup:** Conceptualization, Writing – review & editing. **Lars O. Nord:** Conceptualization, Writing – review & editing, Supervision.

Declaration of Competing Interest

The authors declare that they have no known competing financial interests or personal relationships that could have appeared to influence the work reported in this paper.

Fig. 33. Combined cycle power distribution (SGT-750).

Data availability

Data will be made available on request.

Acknowledgement

This publication has been produced with support from the Low-Emission Research Centre (www.lowemission.no), performed under the Norwegian research program PETROSENTER. The authors acknowledge the industry partners in LowEmission for their contributions and the Research Council of Norway (**296207**).

The Authors express their gratitude to Lennart Naes and Siemens Energy for supplying the industrial data from the Siemens in-house performance model and for their valuable assistance in thoroughly examining the concept.

References

[1] Norwegian Ministry of Climate and Environment, "Norway's National Plan related to the Decision of the EEA Joint Committee," no. 269, 2019.

[2] "Emission to air," Statistics Norway. [Online]. Available: https://www.ssb.no/en/natur-og-miljo/forurensning-og-klima/statistikk/utslipp-til-luft.

[3] I. Sølvberg, "Resource report; discoveries and fields," 2019.

[4] Kjersti Dahle Grov, "Resource Report 2022," 2022.

[5] Torgeir Stordal, "Exploration Resource report 2020," 2020. [Online]. Available: https://www.npd.no/en/facts/publications/reports/resource-report/resource-report-2020/.

[6] International Renewable Energy Agency, "IRENA (2023), Renewable capacity statistics 2023," Abu Dhabi, 2023.

[7] International Renewable Energy Agency, "IRENA (2021), Renewable Power Generation Costs in 2020," Abu Dhab, 2021.

[8] W. Rory O'Sullivan, "Offshore Wind in Europe-Key Trends and Statistics 2020," 2020.

[9] E.O. Jåstad, I.M. Trotter, T.F. Bolkesjø, Long term power prices and renewable energy market values in Norway – A probabilistic approach, Energy Econ. 112 (August) (2021) 2022, https://doi.org/10.1016/j.eneco.2022.106182.

[10] J.I. Marvik, E.V. Øyslebø, M. Korpås, Electrification of offshore petroleum installations with offshore wind integration, Renew. Energy 50 (2013) 558–564, https://doi.org/10.1016/j.renene.2012.07.010.

[11] "Støtte fra Enova til Pionerprosjekt," Equinor. [Online]. Available: https://www.equinor.com/news/archive/enova-supporting-pioneer-project.

[12] T. Burton, D. Sharpe, N. Jenkins, E. Bossanyi, Wind Energy Handbook. (2001).

[13] M.A. Gonzalez-Salazar, T. Kirsten, L. Prchlik, Review of the operational flexibility and emissions of gas- and coal-fired power plants in a future with growing renewables, Renew. Sustain. Energy Rev. 82 (July 2017) (2018) 1497–1513, https://doi.org/10.1016/j.rser.2017.05.278.

[14] G.G. Ol'khovskii, Combined cycle plants: yesterday, today, and tomorrow, Therm. Eng. 63 (7) (2016) 488–494.

[15] M.A. Motamed, L.O. Nord, Part-load efficiency boost in offshore organic Rankine cycles with a cooling water flow rate control strategy, Energy (2022) 124713.

[16] M.A. Motamed, L.O. Nord, Assessment of organic rankine cycle part-load performance as gas turbine bottoming cycle with variable area nozzle turbine technology, Energies (Basel) 14 (23) (2021), https://doi.org/10.3390/en14237916.

[17] K.W. Karstensen, J.O. Wiggins, A Variable-Geometry Power Turbine for Marine Gas Turbines, vol. 112, no. April, 1990.

[18] R. Dutta, L.O. Nord, O. Bolland, Selection and design of post-combustion CO2 capture process for 600 MW natural gas fueled thermal power plant based on operability, Energy 121 (2017) 643–656, https://doi.org/10.1016/j.energy.2017.01.053.

[19] L.O. Nord, O. Bolland, Design and off-design simulations of combined cycles for offshore oil and gas installations, Appl. Therm. Eng. 54 (1) (2013) 85–91, https://doi.org/10.1016/j.applthermaleng.2013.01.022.

[20] L. Pierobon, A. Benato, E. Scolari, F. Haglind, A. Stoppato, Waste heat recovery technologies for offshore platforms, Appl. Energy 136 (2014) 228–241, https://doi.org/10.1016/j.apenergy.2014.08.109.

[21] L. Pierobon, U. Larsen, T. Van Nguyen, F. Haglind, Optimization of organic rankine cycles for off-shore applications, Proc. ASME Turbo Expo vol. 5 B (2013) 1–11, https://doi.org/10.1115/GT2013-94108.

[22] H. Yu, L.O. Nord, J. Zhou, F. Si, Part-Load Performance Analysis of a Combined Cycle Plant Co-Firing Biogas and Natural Gas, 2019.

[23] F. Haglind, Variable geometry gas turbines for improving the part-load performance of marine combined cycles - Combined cycle performance, Appl. Therm. Eng. 31 (4) (2011) 467–476, https://doi.org/10.1016/j.applthermaleng.2010.09.029.

[24] K. Jonshagen, Exhaust Gas Recirculation To Improve Part Load Performance on Combined Cycle Power Plants, in: Proceedings of ASME Turbo Expo 2016: Turbomachinery Technical Conference and Exposition, Seoul, South Korea.

[25] J.H. Kim, T.S. Kim, J.L. Sohn, S.T. Ro, Comparative analysis of off-design performance characteristics of single and two-shaft industrial gas turbines, J. Eng. Gas Turbine Power 125 (4) (2003) 954–960, https://doi.org/10.1115/1.1615252.

[26] A. Wiedermann, M.V. Petrovic, Through-flow modeling of single- and two-shaft gas turbines at wide operating range, Proc. ASME Turbo Expo 2C–2018 (2018) 1–9, https://doi.org/10.1115/GT201875394.

[27] J.C. Cox, D.A. Hutchinson, J.I. Oswald, The Westinghouse/Rolls-Royce WR-21 gas turbine variable area power turbine design. International Gas Turbine and Aeroengine Congress and Exposition, The American Society of Mechanical Engineers, Houston, Texas, 1995.

[28] F. Haglind, Variable geometry gas turbines for improving the part-load performance of marine combined cycles - Gas turbine performance, Energy 35 (2) (2010) 562–570, https://doi.org/10.1016/j.energy.2009.10.026.

[29] Z. Liu, I.A. Karimi, New operating strategy for a combined cycle gas turbine power plant, Energy Convers. Manag. 171 (March) (2018) 1675–1684, https://doi.org/10.1016/j.enconman.2018.06.110.

[30] A.M. Alcaráz-Calderon, M.O. González-Díaz, Á. Mendez, J.M. González-Santaló, A. González-Díaz, Natural gas combined cycle with exhaust gas recirculation and CO2 capture at part-load operation, J. Energy Inst. 92 (2) (2019) 370–381, https://doi.org/10.1016/j.joei.2017.12.007.

[31] S. Ravelli, Thermodynamic Assessment of Exhaust Gas Recirculation in High-Volume Hydrogen Gas Turbines in Combined Cycle Mode, J. Eng. Gas Turbine Power 144 (11) (2022) pp, https://doi.org/10.1115/1.4055353.

[32] M. Ditaranto, H. Li, T. Løvås, Concept of hydrogen fired gas turbine cycle with exhaust gas recirculation: Assessment of combustion and emissions performance, Int. J. Greenhouse Gas Control 37 (2015) 377–383, https://doi.org/10.1016/j.ijggc.2015.04.004.

[33] M. Ditaranto, H. Li, Y. Hu, Evaluation of a pre-combustion capture cycle based on hydrogen fired gas turbine with exhaust gas recirculation (EGR), Energy Procedia 63 (1876) (2014) 1972–1975, https://doi.org/10.1016/j.egypro.2014.11.211.

[34] M. Ditaranto, T. Heggset, D. Berstad, Concept of hydrogen fired gas turbine cycle with exhaust gas recirculation: Assessment of process performance, Energy 192 (2020) 116646, https://doi.org/10.1016/j.energy.2019.116646.

[35] H. Li, G. Haugen, M. Ditaranto, D. Berstad, K. Jordal, Impacts of exhaust gas recirculation (EGR) on the natural gas combined cycle integrated with chemical absorption CO2 capture technology, Energy Procedia 4 (2011) 1411–1418, https://doi.org/10.1016/j.egypro.2011.02.006.

[36] N. Sipöcz, F.A. Tobiesen, Natural gas combined cycle power plants with CO2 capture - Opportunities to reduce cost, Int. J. Greenhouse Gas Control 7 (2012) 98–106, https://doi.org/10.1016/j.ijggc.2012.01.003.

[37] D. Burnes, P. Saxena, P. Dunn, Study of Using Exhaust Gas Recirculation on a Gas Turbine for Carbon Capture. Turbo Expo: Power for Land, Sea, and Air, American Society of Mechanical Engineers, 2020 p. V005T06A034.

[38] Y. Qureshi, U. Ali, F. Sher, Part load operation of natural gas fired power plant with CO2 capture system for selective exhaust gas recirculation, Appl. Therm. Eng. vol. 190, no. March (2021) 116808, https://doi.org/10.1016/j.applthermaleng.2021.116808.

[39] M. Vaccarelli, R. Carapellucci, L. Giordano, Energy and economic analysis of the CO2 capture from flue gas of combined cycle power plants, in: Energy Procedia, Elsevier B.V., 2014, pp. 1165–1174, https://doi.org/10.1016/j.egypro.2014.01.122.

[40] L. Cowell, S. Reynolds, T. Caron, D. Zhang, Demonstration of bleed air recirculation system to improve part load efficiency of solar mars® 100 DLE industrial gas turbine, Proc. ASME Turbo Expo 9 (2018), https://doi.org/10.1115/GT2018-75876.

[41] D. Burnes, P. Saxena, Operational Scenarios of a Gas Turbine Using Exhaust Gas Recirculation for Carbon Capture, J. Eng. Gas Turbine Power 144 (2) (2022) 1–12, https://doi.org/10.1115/1.4052266.

[42] T. Bexten, S. Jörg, N. Petersen, M. Wirsum, P. Liu, Z. Li, Model-Based Thermodynamic Analysis of a Hydrogen-Fired Gas Turbine with External Exhaust Gas Recirculation, J. Eng. Gas Turbine Power 143 (8) (2021) 1–9, https://doi.org/10.1115/1.4049699.

[43] M. Sammak, C. Ho, A. Dawood, A. Khalidi, Improving combined cycle part load performance by using exhaust gas recirculation through an ejector, Proc. ASME Turbo Expo 4 (2021) 1–6, https://doi.org/10.1115/GT2021-59358.

[44] F. Sander, R. Carroni, S. Rofka, E. Benz, Flue gas recirculation in a gas turbine: Impact on performance and operational behavior, in: Proceedings of the ASME Turbo Expo, 2011, pp. 123–132. doi: 10.1115/GT2011-45608.

[45] L.O. Nord, R.M. Montañés, Compact steam bottoming cycles: Model validation with plant data and evaluation of control strategies for fast load changes, Appl. Therm. Eng. 142 (July) (2018) 334–345, https://doi.org/10.1016/j.applthermaleng.2018.07.012.

[46] R.M. Montañés, G. Skaugen, B. Hagen, D. Rohde, Compact Steam Bottoming Cycles: Minimum Weight Design Optimization and Transient Response of Once-Through Steam Generators, Front. Energy Res. 9 (June) (2021) 1–18, https://doi.org/10.3389/fenrg.2021.687248.

[47] M.A. Motamed, L.O. Nord, Development of a simulation tool for design and off-design performance assessment of offshore combined heat and power cycles, in: Proceedings of the 63rd International Conference of Scandinavian Simulation Society, SIMS 2022, Trondheim, Norway, September 20–21, 2022, vol. 192, pp. 1–8, 2022, doi: 10.3384/ecp192001.

[48] I.H. Bell, J. Wronski, S. Quoilin, V. Lemort, Pure and pseudo-pure fluid thermophysical property evaluation and the open-source thermophysical property library CoolProp, Ind. Eng. Chem. Res. 53 (6) (2014) 2498–2508.

[49] H.I.H. Saravanamuttoo, G.F.C. Rogers, H. Cohen, Gas turbine theory, Pearson Education, 2001.

[50] R.M. Plencner, Plotting component maps in the Navy/NASA Engine Program (NNEP): A method and its usage, National Aeronautics and Space Administration no. January (1989).

[51] J. Kurzke, How to get component maps for aircraft gas turbine performance calculations. Turbo Expo: Power for Land, Sea, and Air, American Society of Mechanical Engineers, 1996 p. V005T16A001.

[52] J. Kurzke, I. Halliwell, Propulsion and power: an exploration of gas turbine performance modeling, Springer, 2018.

[53] R.G. Stabe, W.J. Whitney, T.P. Moffitt, Performance of a High-Work Low Aspect Ratio Turbine Tested With a Realistic Inlet Radial Temperature Profile, NASA Tech. Memo. (1984), https://doi.org/10.2514/6.1984-1161.

[54] B.A.L. Hagen, M. Nikolaisen, T. Andresen, A novel methodology for Rankine cycle analysis with generic heat exchanger models, *Appl. Therm. Eng.* 165(October 2019) (2020) 114566, doi: 10.1016/j.applthermaleng.2019.114566.

[55] W.N. Selander, Explicit Formulas for the Computation of Friction Factors in Turbulent Pipe Flow., At Energy Can Ltd AECL Rep, no. 6354, 1978.

[56] P.L. Dhar, Thermal System Design and Simulation, 2016.

[57] K. Jonshagen, M. Genrup, Improved load control for a steam cycle combined heat and power plant, Energy 35 (4) (2010) 1694–1700, https://doi.org/10.1016/j.energy.2009.12.019.

[58] G. Cordes, Strömungstechnik der gasbeaufschlagten Axialturbine. 1963. doi: 10.1007/978-3-642-94859-6.

[59] M. Thern, K. Jordal, M. Genrup, Temporary CO_2 capture shut down: Implications on low pressure steam turbine design and efficiency, vol. 51, no. 1876, 2014, pp. 14–23, doi: 10.1016/j.egypro.2014.07.002.

[60] K. Baumann, Some recent developments in large steam turbine practice, J. Inst. Electr. Eng. 59 (302) (1921) 565–623, https://doi.org/10.1049/jiee-1.1921.0040.

[61] V. Petr, M. Kolovratnik, Wet steam energy loss and related Baumann rule in low pressure steam turbines, Proc. Inst. Mech. Eng. Part A: J. Power Energy (2014) 206–215, https://doi.org/10.1177/0957650913512314.

[62] D. Hu, S. Li, Y. Zheng, J. Wang, Y. Dai, Preliminary design and off-design performance analysis of an Organic Rankine Cycle for geothermal sources, Energy Convers. Manag. 96 (2015) 175–187, https://doi.org/10.1016/j.enconman.2015.02.078.

[63] B. Nazari, M.H. Keshavarz, F. Roohi, Simple method to assess autoignition temperature of organic ether compounds with high reliability for process safety, J. Therm. Anal. Calorim. no. 0123456789 (2021), https://doi.org/10.1007/s10973-021-10846-8.

[64] "MATLAB version R2020b." The MathWorks Inc, 2020.

[65] THERMOFLOW, "GT PRO and GT MASTER." THERMOFLOW INC, 2006. Accessed: Dec. 05, 2023. [Online]. Available: https://www.thermoflow.com/products_gasturbine.html.